Diplomarbeit

Diagnostic value of ^{68}Ga-DOTA-NOC PET/CT in patients with neuroendocrine tumours of the pancreas: a retrospective study

eingereicht von

Evelyn Sebestyen

zur Erlangung des akademischen Grades

Doktorin der gesamten Heilkunde

(Dr.^{in} med. univ.)

an der

Medizinischen Universität Graz

ausgeführt an der

Universitätsklinik für Radiologie

Klinische Abteilung für Nuklearmedizin

unter der Anleitung von

Univ.-Ass. Dr.^{in} Susanne Stanzel

und

Univ.-Prof. ^{in} Dr.^{in} Reingard M. Aigner

Graz, am 25.06.2019

Eidesstattliche Erklärung

Ich erkläre ehrenwörtlich, dass ich die vorliegende Arbeit selbstständig und ohne fremde Hilfe verfasst habe, andere als die angegebenen Quellen nicht verwendet habe und die den benutzten Quellen wörtlich oder inhaltlich entnommenen Stellen als solche kenntlich gemacht habe.

Graz, am 25.06.2019 *Evelyn Sebestyen eh*

Danksagungen

Mein größter Dank gilt zu Beginn meiner Erstbetreuerin Frau Univ.-Ass. Dr.in Susanne Stanzel, die mich in meiner Arbeit fachlich und geduldig unterstützt hat sowie Frau Univ.-Prof.in Dr.in Reingard Aigner. Herrn Dipl. Ing. Dr. Kvaternik danke ich für sein Engagement im Wahlfach, das mich zu dieser Diplomarbeit geführt hat. An dieser Stelle möchte ich Herrn Mag. Dr. Quehenberger für seine fachliche Unterstützung in der statistischen Auswertung dieser Arbeit danken.

An dieser Stelle möchte ich mich von ganzem Herzen bei meinen Eltern bedanken, die mir dieses Studium fernab der Heimat überhaupt ermöglicht haben. Einen besonderen Dank möchte ich an meine liebe Mutter hervorheben, da sie während der gesamten Studienzeit für mich die größte mentale Unterstützung war und man sich als Kind viel zu selten bedankt. In diesem Sinne: mersi pentru tot cu toata dragostea draga Mama.

Abschließend gilt ein großes Dankeschön an meine Freunde, die meine Studienzeit unvergesslich gemacht und bereichert haben, sowie zum Schluss meinem Freund Fabian, der immer ein offenes Ohr für meine Anliegen hat und mich in jeder Hinsicht liebevoll unterstützt.

Zusammenfassung

Gegenstand

Das Ziel dieser retrospektiven Studie ist die Evaluierung der Bedeutung von ^{68}Ga-DOTA-NOC in der Diagnostik von histologisch gesicherten neuroendokrinen Tumoren im Pankreas (pNET).

Methode

^{68}Ga-DOTA-NOC PET/CT Aufnahmen von 30 Patienten/Innen mit histologisch gesichertem NET des Pankreas wurden ausgewertet. Die Aufnahme des Tracers im Pankreas und in Fernmetastasen wurde quantifiziert und mittels Messung des SUV_{max} (maximum standardized uptake value) miteinander verglichen. Ein cut-off Wert des SUV_{max} zur Unterscheidung des physiologischen vom pathologischen Tracer-Uptake im Pankreas wurde mittels ROC-Analyse ermittelt. PET/CT Bilder wurden in Hinblick auf detektierte Läsionen gesamt und einzeln pro Patient/in (Läsionen-basierte Analyse) untersucht, sowie die Anzahl der Patienten/Innen mit identifiziertem Primärtumor und Fernmetastasen (Patienten/Innen-basierte Analyse) bestimmt. Die Ergebnisse wurden mit Detektionsraten herkömmlicher Tracer (^{18}F-FDOPA, ^{111}In-Octreotid, ^{99m}Tc-HYNIC-TOC und ^{18}F-FDG) aus der Literatur verglichen. Die regionale Speicherintensität der Läsionen wurde mittels Messung des SUV_{max} quantifiziert und ein cut-off Wert über dem Pankreas ermittelt.

Ergebnisse

Die Histologie ergab 16 Fälle an gut differenzierten pNET (G1), 12 Fälle an mäßig differenzierten (G2), einen Fall an schlecht differenziertem pNET und einen Fall mit gesicherter Histologie eines pNETs, jedoch ohne Tumorgrading. Von diesen Patienten/Innen hatten 20 eine oder mehrere pathologische ^{68}Ga-DOTA-NOC metabolisierende Läsionen, wovon bei 12/20 Patienten/Innen ein Primum im Pankreas detektiert werden konnte. Hierbei war bei 7/12 (58%) Patienten/Innen die Cauda pancreatis am häufigsten betroffen. Die verbleibenden 10 Patienten/Innen hatten einen unauffälligen Befund. Basierend auf den histopathologischen Ergebnissen und multiplen follow-up Untersuchungen betrug die Patienten/Innen-basierte Sensitivität, Spezifität und diagnostische Genauigkeit für die ^{68}Ga-DOTA-NOC PET/CT jeweils 100%. Ebenso betrug die Läsionen-basierte Sensitivität, Spezifität und diagnostische Genauigkeit sowohl für die identifizierten 15 Pankreasläsionen als auch für sämtliche detektierte Fernmetastasen (n=253) jeweils 100%. Laut Literatur

beträgt die Sensitivität der SRS (Somatostatin Rezeptor Szintigrafie) mit ^{111}In-Octreotid und ^{99m}TC-HYNIC-TOC sowie der ^{18}F-FDOPA und ^{18}F-FDG-PET/CT für pNETs jeweils weniger als 50-60%, 87%, 80% bzw. 60% und liegt somit deutlich unter jener der ^{68}Ga-DOTA-NOC PET/CT. Der berechnete cut-off Wert des SUV_{max} ergab 23,27 bei einer Sensitivität von 100% und einer Spezifität von 60%. Außerdem konnten signifikante Unterschiede des medianen SUV_{max} in Hinblick auf Geschlecht, Funktionalität, Ki-67 Index, sowie nach 2010 WHO Grading innerhalb der pathologischen Befunde festgestellt werden.

Schlussfolgerung

Der Somatostatinrezeptor(2,3,5)-spezifische Tracer ^{68}Ga-DOTA-NOC detektiert signifikant mehr Läsionen in gut differenzierten pNETs mit positivem Somatostatinrezeptor Status. Er weist eine höhere Genauigkeit als andere verfügbare Tracer für die Detektion und das Staging neuroendokriner Tumore des Pankreas auf. ^{68}Ga-DOTA-NOC sollte als Goldstandard in der nuklearmedizinischen Bildgebung für pNETs angesehen werden.

^{18}F-FDOPA ist geeigneter für gut differenzierte Tumore mit niedrigen oder variablen Somatostatinrezeptor Status. ^{18}F-FDG ist die beste Wahl für schlecht differenzierte neuroendokrine Tumore im Pankreas.

Abstract

Objective

The aim of this retrospective study is to evaluate the diagnostic value of ^{68}Ga-DOTA-NOC PET/CT in patients with histologically confirmed neuroendocrine tumour of the pancreas (pNET).

Methods

^{68}Ga-DOTA-NOC PET/CT scans of thirty patients with proven pNETs were evaluated. The tracer uptake in the pancreas and distant lesions were quantified and compared by measuring the maximum standardized uptake value (SUV_{max}). A cut-off value of SUV_{max} to differentiate between physiological and pathological tracer-uptake in the pancreas was obtained by using ROC-analysis. PET/CT scans were analysed in terms of detected lesions in total and per patient (lesion-based analysis), and patients with identified primary tumour and distant metastases (patient-based analysis). The results were compared to detection rates of commonly used tracers such as ^{18}F-FDOPA, ^{111}In-octreotide, ^{99m}Tc-HYNIC-TOC, and ^{18}F-FDG in literature. The local tracer uptake was measured with SUV_{max}, and a pancreatic cut-off value was determined.

Results

Histology revealed low-grade pNET (G1) in 16 patients, intermediate grade (G2) in 12, high-grade (G3) in 1, and one patient had confirming histology of a pNET but without indication of the tumour grading. Twenty patients had pathological ^{68}Ga-DOTA-NOC metabolic lesions; of these, in 12 a primary lesion in the pancreas was identified. Here in 7/12 patients (58%), the cauda pancreatis was most commonly affected. The other 10 patients were without pathological findings. Based on the histopathological findings and multiple follow-ups, the patient-based sensitivity, specificity, and diagnostic accuracy for ^{68}Ga-DOTA-NOC PET/CT were each 100%. The lesion-based sensitivity, specificity, and diagnostic accuracy for 15 pancreatic lesions and 253 distant metastases were 100%, respectively. Thus, according to literature the sensitivity of SRS (somatostatin receptor scintigraphy) with ^{111}In-octreotide or ^{99m}Tc-HYNIC-TOC as well as ^{18}F-FDOPA and ^{18}F-FDG PET/CT for pNETs was with less than 50-60%, 87%, 80%, and 60%, respectively significantly lower than that of ^{68}Ga-DOTA-NOC PET/CT calculated in the present study. The calculated cut-off value of SUV_{max} is 23.27 in this study with a sensitivity of 100% and specificity of 60%.

Furthermore, there were significant differences of the median SUV_{max} with regard to sex, functioning, Ki-67 index, and 2010 WHO classification within the pathological ^{68}Ga-DOTA-NOC results.

Conclusion

The SSR-2,3,5-specific tracer ^{68}Ga-DOTA-NOC detects significantly more lesions, and with higher accuracy, in well-differentiated pNETs with positive somatostatin receptor (SSR) expression than any other tracer used for the detection and staging of neuroendocrine tumours of the pancreas. ^{68}Ga-DOTA-NOC should be considered as the gold standard for functional nuclear imaging of pNETs.

^{18}F-FDOPA is more suitable for well-differentiated tumours with low or variable SSR expression. ^{18}F-FDG appears to be the best option for high-grade pNET.

Table of contents

1 Glossary and abbreviations

ATRX	Alpha-Thalassemia/Mental Retardation Syndrome X-Linked
°C	degree Celsius
C18	carbon18
CGA	Chromogranin A
Ci	curie
cm^3	cubic centimetre
C-peptide	connecting peptide
CT	computerised tomography
DAXX	death domain-associated protein
DNA	deoxyribonucleic acid
DOTA	1,4,7,10-Tetraazacyclododecane-1,4,7,10-tetraacetic acid; Tetraxetan
e.g.	exempli gratia; for example
et al.	et allii/aliae, and other authors
^{18}F	Fluoride ion
FDG	fluorodeoxyglucose
F-DOPA	fluorinated L-3,4-dihydroxyphenylalanine/L-DOPA
G	grade
g	gram
Ga	Gallium
Ge	Germanium
GLP-1	Glucagon-like Peptide 1
GMP	good manufacturing practice
H^+	hydrogen cation
HCl	hydrochloric acid
HEPES	4-(2-hydroxyethyl)-1-piperazineethanesulfonic acid
HPF	high power field
HPLC	high-performance liquid chromatography
HYNIC	hydrazinonicotinic acid
IAEA	International Atomic Energy Agency
In	Indium
IQR	interquartile range
IU	international unit

keV	kilo-electronvolt
Ki-67	Ki (Kiel)-67 protein
l	litre
LAL	Limulus amebocyte lysate
Lnn.	lymph nodes
M	molar mass
Max.	maximum
MBq	mega becquerel (1MBq = 0.027 mCi)
MEN1	multiple endocrine neoplasia, type 1
mg	milligram
MIBG	metaiodobenzylguanidine
min	minute
MIP	maximum intensity projection
ml	millilitre
mm	millimetre
mmol/l	millimoles per litre
MRCP	magnetic resonance cholangiopancreatography
MRI	magnetic resonance imaging
mSv	milliSievert
(m)TOR	(mammalian) target of rapamycin
µg	microgram
µm	micrometer
n	sample size
N_2	dinitrogen, nitrogen gas
NaCl	sodium chloride
nM	nanomolar
No.	number
NOC	NaI^3-octreotide
NSE	neuron-specific enolase
P	probability value
PBS	phosphate buffered saline
PET	positron emission tomography
pH	unit to specify the acidity/basicity of aqueous solution; logarithmic scale

Ph. Eur.	European Pharmacopoeia
pNET	pancreatic neuroendocrine tumour
PP	pancreatic polypeptide
PRRT	peptide receptor radionuclide therapy
PTEN	Phosphatase and tensin homolog
ROC	Receiver Operating Characteristic
ROI	region of interest
SC	cassette system
SPE	solid phase extraction
SPECT	single-photon emission CT
SRS	somatostatin receptor scintigraphy
SSR	somatostatin receptor
SST	somatostatin
SUV_{max}	maximum standardized uptake value
TATE	Octreotide/somatostatin analogue; Tyr3
^{99m}Tc	Technetium exametazime
TLC	thin-layer chromatography
TM	trademark
TOC	Octreotide/somatostatin analogue; D-Phe1-Tyr3
TSC2	Tuberous Sclerosis Complex 2
V	volume
VHL	von Hippel-Lindau syndrome
VIP	vasoactive intestinal peptide
v/v	volume/volume
vs.	versus
WHO	World Health Organization
y	year(s)

2 List of figures and tables

3 Introduction

3.1 Pancreas

3.1.1 Anatomy

The pancreas is built up of proper lobules, which are connected by loose areolar tissue that also surrounds the entire organ. Each lobule is comprised of tubular alveoli, that are nearly entirely filled with secretory cells. The ducts of each of the lobules converge to form the pancreatic duct.

The pancreas is anatomically structured in three parts: the right extremity, being quite ample, is named the head (caput), with a dorsal mass specified as uncinate process, and is confluent with the body (corpus), which forms the majority of the pancreas. The tapered end of the organ is known as the tail.

The length as well as the weight of this organ varies from 12.5-15 cm and accordingly from 60-100 g [1].

3.1.2 Physiology

The pancreas has two main functions: it serves as an exocrine organ with secretions to aid digestion, and an endocrine function with secretion of the hormones insulin and glucagon.

The pancreatic juice flows out to the duodenum through the pancreatic duct. The digestive enzymes cause the splitting of carbohydrates, fats, and proteins in the intestine.

The endocrine function of the organ is performed by the islets of Langerhans, which are comprised of connective tissue between the alveoli. These islets feature two types of cells: A cells, which produce glucagon and B cells, the origin of insulin. Both hormones play a key role in regulating glucose homeostasis [1].

3.2 Neuroendocrine tumour of the pancreas

Neuroendocrine tumours arise from pancreatic islet cells. Hence, the preferred terminology is *pancreatic neuroendocrine tumour*, *panNET,* or just simply *pNET*.

In comparison with other tumours, which arise from the exocrine part of the organ, pNETs are rare and represent only about 2% of all pancreatic neoplasms [2]. The controversial incidence is illustrated by the fact that pNETs can be found in about 1% of autopsies, the clinical incidence referred to be only about 0,5-1/100.000 [3].

3.2.1 Types

Any part of the pancreatic mass, as well as the surrounding peripancreatic tissue, can be affected by the tumour. Carcinoid tumours can imitate their original histological counterparts, which are located elsewhere in the body. As with any other neoplasm, pNETs can appear as single or multiple, and be benign or malignant [2].

Pancreatic NETs are classified as non-functional or functional (table 1). Clinical syndromes, caused by functional pNETs, arise out of hormone hypersecretion related to the cell of origin (e.g., insulin, gastrin, glucagon or vasoactive intestinal peptide). Inherited genetic syndromes can also predispose to pNETs and are associated with them in some cases [4].

Table 1: Types of pancreatic NETs [2] [5] [6] [7]

An overview of all types is given by naming the main clinical symptoms, location, and essential markers.

Type	Clinical feature	Location of tumour	Biomarker
Insulinoma	Hypoglycaemia, confusion, stupor	any part of the organ	Insulin, proinsulin, C-peptide
Gastrinoma	Diarrhoea, severe peptic ulceration	Gastrinoma triangle	Gastrin, PP
VIPoma	Watery diarrhoea, hypokalaemia, achlorhydria	body and tail	VIP
Glucagonoma	Mild diabetes mellitus, anaemia, necrolytic migratory erythema	body and tail	Glucagon, glycentin
Somatostatinoma	Diabetes mellitus, cholelithiasis, steatorrhea, hypochlorhydria	pancreatoduodenal groove, ampullary, periampullary	Somatostatin
Pancreatic carcinoid	Abdominal pain, diarrhoea	any part of the organ	Serotonin
PPoma	Steatorrhea	head	PP

3.2.2 Signs and Symptoms

Most patients with pancreatic neoplasm initially present with similar symptoms: abdominal pain, weight loss, jaundice, splenomegaly, or gastrointestinal bleeding. Lesions in the head of the pancreas may cause jaundice due to its obstructive character, whereas lesions in body and tail may result in the before mentioned splenomegaly by reason of splenic vein obstruction.
Pancreatic NETs may destroy the surrounding physiological tissue and/or glandular structures, leading to diabetes, or loss of pancreatic exocrine function [1].

The indolent nature of pNETs is described in clinical cases as a dissociation from the more common pancreatic adenocarcinomas. The aggressiveness of this tumour has a few influencing factors: tumour load, grade of malignancy, metastases (regional and/or distant), vascular invasion, and local infiltration [8].

Non-functional neoplasms, which are more common, can lead to biliary obstruction, haemorrhage, or abdominal masses; and functional represent the consequences of the overproduced hormone with an endocrine syndrome [1].

3.2.3 Diagnosis

Helical and multiphase computed tomography (CT) and magnetic resonance cholangiopancreatography (MRCP) are used as standard imaging methods for pancreatic cancer. Maximum contrast enhancement is seen in the late arterial phase.
Laboratory tests may be performed initially but are often non-specific and do not aid diagnosis [1] [4]. However, endocrine testing should be considered to differentiate between functional and non-functional pNETs [9]. CT or endoscopic ultrasound guidance is necessary for fine-needle aspiration to obtain tissue for definitive diagnosis [1].
The aim of all diagnostic methods is to reflect the nature of cancer: tumour grade and its primary, status of metastases, and endocrine function.
Tumour markers, such as Chromogranin A (CGA), neuron-specific enolase (NSE), and pancreastatin can also be used for follow-up evaluation, as well as hypersecreted hormones in functional pNETs.
It happens that imaging leads to no result, what may occur in circumstances of occult tumours. In this case, nuclear imaging with octreotide is absolutely indicated. This also has the added benefit of assessing the affinity of the pNET for somatostatin [9] [10].

Recently, a new positron-emitting radionuclide, ^{68}Gallium, has become the gold standard for PET/CT imaging to detect small pNETs and their metastases. ^{68}Gallium is attached via chelators (e.g. DOTA) to biomolecules, which bind to the receptor presented by the tumour cells [4].

3.2.4 Staging

According to the 2010 World Health Organization (WHO) classification, pNETs are graded in three categories [11]:

Table 2: 2010 WHO Grading of NETs

Grade	Mitotic count[1]	Ki-67 Index	Differentiation
G1	<2	≤2	well-differentiated
G2	2-20	3-20	moderately differentiated
G3	>20	>20	poorly differentiated

[1]10 HPF (high power field) = 2mm^2

Gastroenteropancreatic NET staging is based on the criteria of the European Neuroendocrine Tumour Society and the American Joint Committee on Cancer/Union for International Cancer Control [12] [13].

3.2.5 Genetics

Sporadic pNETs show repetitive somatic alterations in their DNA. Three major genes or pathways must be pointed out [2]:

- *MEN1*, which generates familial MEN syndrome, type 1.
- *PTEN* and *TSC2:* These are tumour suppressor genes with loss-of-function mutations. This leads to the oncogenic mammalian TOR (mTOR) signalling pathway.
- Alpha-thalassaemia, X-linked (*ATRX*) and *DAXX*: About 50% of pNETs appear with a somatic mutation concerning the first or the second mentioned inactivating mutation. Various functions are coded by these genes, to distinguish the telomere maintenance.

Although decoding the genetic sequences of pNETs has been the target of numerous studies, the exact signalling pathway caused by mutations remains largely elusory. While most cases are sporadic, three hereditary syndromes are associated with pNETs: Multiple Endocrine

Neoplasia type 1 (MEN1), von Hippel-Lindau (VHL) and von Recklinghausen's disease (Neurofibromatosis 1) [14].

Table 3: Hereditary Syndromes and their characteristics [14]

Hereditary syndromes vary in genetics and the features of occurring pNET.

Syndrome	Gene Locus	Tumour Character
MEN1	11q13	Mostly non-functional, 80-100% of incidence, extrapancreatic localisation possible
VHL	3p25.5	Somatostatinoma, 12-17% occur in the pancreas
von Recklinghausen's disease	17q11.2	6% in the pancreas

In all cases of neuroendocrine tumours, it is necessary to take a detailed family history and clinically examine the patient to exclude complex cancer syndromes (e.g. MEN1) [15].

3.2.6 Treatment

Treatment paradigms have shifted to more aggressive regimes in the last decade due to specialised teams for the management of pNETs. First, the patient must be interdisciplinarily introduced to evaluate the best curative strategy. Specialists from different sections are integrated to ensure the best outcomes: endocrinologists, oncologists, surgeons, nuclear physicians, and many others.

The ideal treatment plan consists of four main therapies: debulking surgery, locoregional therapy, systemic therapy, and follow-up.

Clinical cure is only possible by excision of the primary tumour and its metastases, especially functional liver metastases. Locoregional methods, such as chemoembolisation, radiofrequency ablation, and other options, should be considered for patients with liver metastases. If surgery and locoregional therapy fail, systemic therapy would follow. The common chemotherapeutic agents are somatostatin analogues or, in rare cases, interferon alpha [9]. Somatostatin analogues as a treatment for non-functioning pNETs are not established yet. Further investigation is required [15].

Intermediate or high-grade pNETs require chemotherapy (e.g. cisplatin or temozolomide), which may provoke severe side-effects. A controversially discussed treatment option in

literature is liver transplantation for patients with predominantly liver metastases. The focus of attention is post-transplantation immunosuppression, which may increase the risk of new non-hepatic metastatic disease [9].

Treatment with somatostatin analogues does not have any influence on PET/CT imaging (e.g., with ^{18}F-FDG) [15].

PET/CT with ^{68}Ga-DOTA-NOC-peptides can detect all types of NETs overexpressing somatostatin receptors on their cell surface, and therefore can be used to select patients for whom peptide receptor radionuclide therapy (PRRT) is appropriate. PRRT has been successfully used as targeted therapy with radionuclides which are linked to somatostatin analogues in patients with inoperable or symptomatic NETs. The most common radionuclides are ^{90}Yttrium or ^{177}Lutetium and DOTA-TOC, DOTA-TATE, DOTA-lanreotide, or DOTA-NOC as a used peptide [3] [16] [17]. Possible side effects of this treatment method are temporary myelosuppression and radiation nephritis, which may be life-threatening [15].

3.2.7 Prognosis

Current studies demonstrate that tumour grade is the safest factor for obtaining information about the future behaviour of pNET. Because of this, the histopathological examination has a high relevance [9]. G3 neoplasms show more aggressive expansion than well-differentiated pNETs [8].

The overall survival rate for all types of cancer in the pancreas is only 6%, resulting in a devastating outcome for patients. The best prognosis and chance of cure is resection of the whole tumour. Nevertheless, only 30% of primary tumours in the head of the pancreas, and a disappointing 10% of those in body or tail, can be totally resected in the first instance [1]. Norwegian and American epidemiological studies have demonstrated the poor prognosis of pNETs: the 5-year survival rate of pancreatic primaries is 27-43% [15].

3.3 Somatostatin

The pancreas has different sorts of cell types. Delta Cells are producing the pancreatic somatostatin with a half-life of 2-3 minutes. This hormone is involved in regulating carbohydrate, fat, and protein metabolism. Somatostatin acts antagonistically to insulin, glucagon and pancreatic polypeptide by inhibiting their release within the islets. Pancreatic

somatostatin varies in function and chemical structure compared to its hypothalamic counterpart [18].
Six human subtypes of somatostatin receptors (SSRs) have been identified (1, 2A, 2B, 3, 4 and 5); some are overexpressed in pNETs compared to normal pancreatic tissue [4] [19]. The highest overexpression shows SSR2 and is utilised by ^{68}Ga-DOTA-peptides, labelled with its positron emitting radionuclide, due to their high affinity [4].

For clinical use, somatostatin analogues with longer half-lives have been generated. SSR can be found in 75-95% of NETs but are less common in insulinomas (50-60%), poorly differentiated NETs and somatostatinomas. Somatostatin analogues inhibit the release of pancreatic peptide hormones by binding to the appropriate receptor and antagonising the effects of the human growth factor. This pathway of somatostatin may induce apoptosis at high dosage [15].

4 Material and Methods

4.1 Study population

This retrospective study includes 30 patients (16 men and 14 women; median age 62 y; IQR 53-69 y) with histologically proven NET of the pancreas (G1, G2 or G3; 2010 WHO classification). PET/CT scans of the years 2015-2017 with ^{68}Ga-DOTA-NOC at the Division of Nuclear Medicine in Graz were analysed in terms of identified lesions per person (lesion-based analysis) and number of patients with detected primary and/or metastases (patient-based analysis).

The additional inclusion criteria were patients who already underwent surgery, obtained peptide receptor radionuclide therapy (^{177}Lutetium-DOTA-TATE), chemotherapy (Rituximab with Bendamustin), or somatostatin therapy before or during the study. The maximum time of follow-up was 16 months. All patients received a physical examination before diagnosis, and their clinical history was investigated with the aim of classifying them into one of the groups mentioned above in terms of diverse therapy. Laboratory and radiologic examinations were performed in advance to evaluate the location and stage of the tumour. Patients were also divided into groups according to the Ki-67 index, histological grading, functioning, and sex. Patients who showed clinical symptoms in combination with an increase in serum peptide levels of insulin or glucagon were identified as functioning tumours. For the purpose of this study, patients were excluded if they had other types of neuroendocrine tumour or had no histology result.

No written informed consent to participate anonymously in this study was necessary due to the study design. The study protocol was approved by the local Ethical Committee of the Medical University of Graz and was performed according to the Helsinki Declaration for human studies.

4.1.1 PET scans

Whole body PET/CT scans are necessary to determine pNETs with ^{68}Ga-DOTA-NOC. The scans are produced in cooperation of two different scanners: the Biograph^{TM}mCT (Siemens Healthineers) and GE Discovery ST PET/CT (GE Healthcare Company).

This sort of imaging is used to detect primary tumours, for follow-ups and to select patients for high-dose therapy.

Before scanning, patients had to sign the declaration of consent and obtained the individually calculated dose of ^{68}Ga-DOTA-NOC. The dose is dependent on the patient's weight. In this

study, the mean dose of 148 MBq (IQR 118-178 MBq) was received through an intravenous injection. The radiopharmaceutical conjugated peptide was capped at a maximum dose of 50µg to avoid any clinically significant side effects. The images were obtained 60 minutes post injection. Patients were required to empty their urinary bladder and remove metallic objects from the body, such as a belt or piercing, prior to scanning.

The shooting mode is static, and the scan mode is three-dimensional. The whole examination includes six bed positions. Each of them takes 150 seconds and requires another 150 seconds per position for acquisition. Approximately two hours are needed for this image examination, including all process steps from consultation until image editing [18]. CT images were used for nonuniform attenuation correction. All images were corrected for scattering, randoms, dead time, and decay. Images were reconstructed with a 2-dimensional ordered-subset expectation maximisation iterative algorithm (2 iterations, 21 subsets). PET/CT images were acquired from the orbital roof to the subinguinal groin as a whole-body scan [3].

4.1.1.1 ^{68}Ga-DOTA-NOC

4.1.1.1.1 Characteristics of ^{68}Ga-DOTA-NOC

^{68}Ga-DOTA-NOC is a complex of ^{68}Gallium with DOTA-[NaI^{3}]-octreotide. The radionuclide ^{68}Gallium has a physical half-life of 68 minutes. The compound is a somatostatin receptor ligand, labelled with the radionuclide ^{68}Ga, with a high affinity for SST receptor subtypes 2, 3 and 5. They are overexpressed by gastroenteropancreatic neuroendocrine tumours (functioning and non-functioning). After injecting the radioactive ^{68}Ga-DOTA-NOC solution intravenously, the distribution can be illustrated by positron emission tomography. PET offers higher resolution in comparison to SST receptor scintigraphy [20] [21].

Good diagnostic tolerance is observed in human use. There are a few cases where side effects, such as hypo- or hypertension, rashes, vomiting, or fever, have been documented. Accessibility is given by a portable ^{68}Ge/^{68}Ga generator – no need of an onsite cyclotron anymore. ^{68}Ga-DOTA-NOC runs through the liver during the elimination process and is finally excreted via urine and impresses with lower doses to human organs compared to SRS tracer [23].

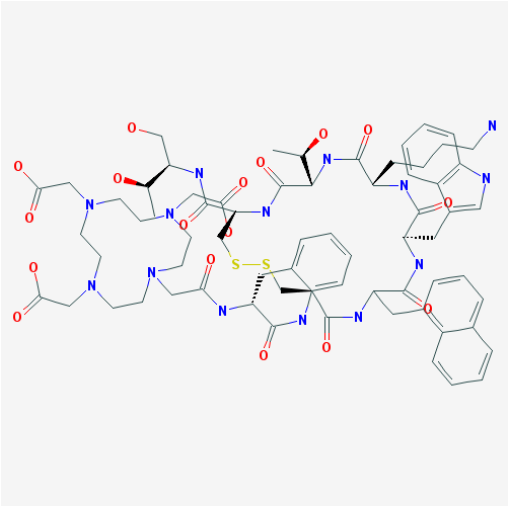

Figure 1: Chemical structure of ^{68}Ga-DOTA-NOC [22]

4.1.1.1.2 Synthesis of ^{68}Ga

The radionuclide ^{68}Ga for labelling can be obtained from a ^{68}Ge/^{68}Ga radionuclide generator (e.g. iThemba Labs (Faure, South Africa) or Eckert & Ziegler (Berlin, Germany)). The mother radionuclide ^{68}Germanium has a half-life of 271 days, which is available in the generator immobilised on an inert matrix of titanium oxide or tin oxide. The daughter ^{68}Ga is continuously produced due to radioactive decay of ^{68}Ge under electron capture. The mother ^{68}Ge is irradiated by stable ^{69}Ga with accelerated protons [24]. The process of eluting the new gathered ^{68}Ga-chloride is done with pure hydrochloric acid. This step happens directly on the way into the hardware out of the generator, which has approximately a service life of a year.

Each contamination would interrupt the following labelling. Metal ions must be eliminated by leading the eluate over a cationic ion exchanger. Only ^{68}Ga(III)-chloride overcomes this wash-out step; other metal ions are gone. The final step is to transfer the pure ^{68}Ga(III)-chloride with the help of 5 M NaCl into the vial for the reaction [25].

4.1.1.1.3 Labelling DOTA-NOC with ^{68}Gallium

The labelling of ^{68}Ga-DOTA-NOC should be immediately before use. The exact radioactivity of ^{68}Ga-DOTA-NOC is dependent on the ^{68}Ga of the generator. The main factors for the level of radioactivity are the actual value of generator strength and the decay factor of the mother radionuclide ^{68}Ge. The generator cannot be eluted partially. Therefore, it provides the total accessible radioactivity [25]. For safety, ring dosimeters are mandatory for nuclear medicine personnel during synthesis and injecting. Studies have shown that doses

are within permissible limits. Each labelling must be documented in the list of charges, in the protocol of the institute and several specific documents, given by the correspondent company of the used item (Scintomics GRP logbook, report of GRP module) [26].

The process of labelling is carried out by a synthesis module GRP™ (Scintomics GmbH, Lindach, Germany) with a cassette system (SC-01 kit, ABX™, Radeberg, Germany), which includes a C-18 cartridge, a PSE®-cartridge, a sterile filter (0,22 µm) and the reagents. The cassettes are manufactured under sterile and GMP conditions. This cassette is for single use; therefore, no cleaning of it and the GRP module ™ is necessary.
The synthesis was performed automatically [27] [28]. The eluate $^{68}Ga^{3+}$ in 1.0 M HCl of a $^{68}Ge/^{68}Ga$-generator (iThemba, Faure, South Africa) was transferred to a cation exchange cartridge Chromafix™ PS-H^+ (Machery-Nagel, Dürren, Germany) and eluted with a mixture of acidified 5 M NaCl. The solution was added to 3 ml 1.5 M HEPES/HCl reaction buffer containing the precursor 40 µg DOTA-NOC (ABX, Radeberg, Germany), maintaining the pH between 3.0 to 3.5 in the reaction mixture. The ^{68}Ga peptide was labelled at 120 °C / 6 minutes. The sequence transferred the reaction mixture onto a Sep-Pak® C18 cartridge. The C18 SPE cartridge was flushed extensively with water. The immobilised ^{68}Ga-DOTA- NOC was then eluted with 2 ml water/ethanol 50/50 (v/v), and then passed through a 0.22 µm sterile filter into a sterile vial and was diluted with PBS buffer to a total volume of 16 ml.

4.1.1.1.4 Pharmaceutical formulation of ^{68}Ga-DOTA-NOC

The result of this labelling is a sterile, pyrogen-free, isotonic, and diluted solution for intravenous injection. The final solution is composed of:

- max. 40 µg of active ^{68}Ga-DOTA-NOC
- phosphate buffered saline
- max. 10% (v/v) of ethanol (Ph. Eur.)

The maximum recommended dose of ^{68}Ga-DOTA-NOC must be less than 50 µg in each patient dose to avoid any clinically significant pharmacological effect (Ph. Eur. No. 2482). A minimum amount of ^{68}Ga-DOTA-NOC solution, conditional of manufacturing, is about 16 ml [29].

4.1.1.1.5 Quality control of ^{68}Ga-DOTA-NOC

The quality control of ^{68}Ga-DOTA-NOC follows international guidelines [30] and the European Pharmacopoeia [29] as legal groundwork for the use of this radiopharmaceutical

on patients. A maximum volume of 5ml, an activity for adults between 111-333 MBq, a minimum activity concentration at the end of the synthesis of 22,2 MBq/ml, and a storage life up to 3 hours after synthesis are defined.

Table 4 gives a summary of the mandatory tests and their limiting values to release the ^{68}Ga-DOTA-NOC solution for human diagnostic purpose. The tests are based on the general monograph Ph. Eur. No. 0125 and the monograph Ph. Eur. No. 2482. The limiting values are referred to the maximum volume (V) of a patient dose.

Table 4: Overview of mandatory tests for final release [29] [30]

Tests	Method	Specifications
identity of radionuclide	gamma spectrometry	480-540 keV
half-life of radionuclide	dose calibrator	62-74 min
identification:^{68}Ga-DOTA-NOC	HPLC	relative retention (^{68}Ga-DOTA-NOC/DOTA-NOC) = about 1.3
pH	indicator strip	4.0-8.0
appearance	visual examination	clear, colourless solution
purity of ^{68}Ga-DOTA-NOC	HPLC	≥ 91.0 %
impurities: colloidal ^{68}Ga, ^{68}Ga(III)ions	HPLC, TLC	≤ 5.0 %
DOTA-NOC and metal complexes	HPLC	≤ 50 µg/V
radionuclide impurity: ^{68}Ge	analysis of decayed sample	< 0.001 %
chemical impurity: HEPES	HPLC	≤ 200 mg/V
excipient: ethanol	gas chromatography	≤ 10 %
bacterial endotoxins	LAL test	≤ 175 IU/V
sterility	direct inoculation	sterile

4.2 PET image evaluation

PET/CT scans were evaluated by skilled nuclear medicine specialists blinded to previous imaging studies to obtain the correct overview of the patient's tumour status. Each localisation which showed a non-physiological intensity superior to background was determined as a pathological lesion, either primum or metastasis. The SUV_{max} and the

volume of each pathological lesion as well as in the pancreatic head was measured by selecting the region of interest with the highest tracer uptake.

Somatostatin receptors are expressed by several neuroendocrine and non-neuroendocrine body cells and can be imaged in the same scintigraphy. This fact is notable since many organs show a physiological tracer-uptake (normal biodistribution). Physiological tracer uptake had to be considered, such as in the pituitary gland, spleen, liver, adrenal glands, salivary glands, thyroid, stomach wall, bowel, kidneys, and urinary bladder (figure 2 and 3). Pancreatic uptake that was linearly and not focally restricted was rated as a physiological finding.

Even though the pancreas expresses all subtypes of SST receptors, it is predominated by SST receptor 2, which is mostly located in the islets. Physiological tracer uptake is found in the pancreas in focal areas, especially in the pancreatic head. This may mimic focal tumour disease, and must be considered in the evaluation [3] [20].

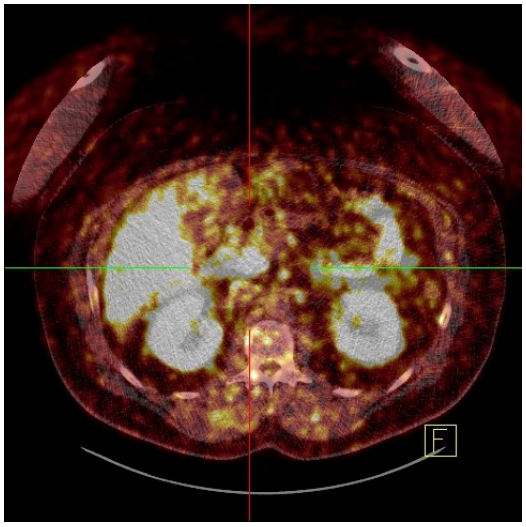

Figure 2: High physiological tracer uptake in PET/CT

The figure shows high uptake in the kidneys, pancreatic head, liver, and adrenal glands.

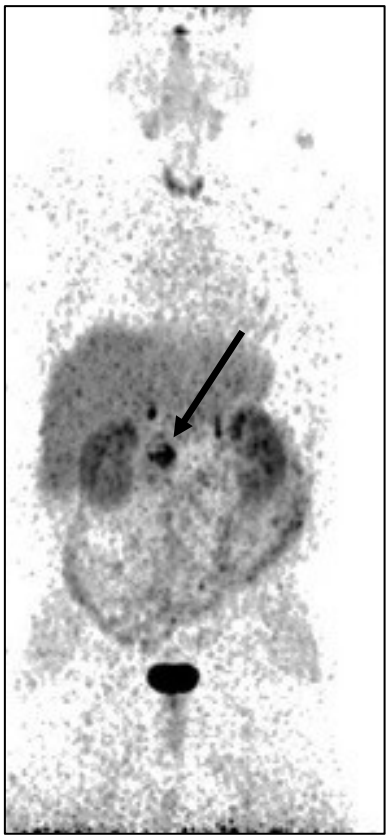

Figure 3: Maximum intensity projection (MIP) of PET/CT with high physiological uptake in the urinary tract and moderate physiological uptake in the pancreatic uncinate process (arrow)

4.3 Statistics

All data were collected, and a computerised data sheet in Microsoft® Office Excel was created. Data on demographic, clinical, and pathologic features were retrospectively analysed. Median values and the respective interquartile ranges (IQR, 25^{th}-75^{th} percentile) were used to describe the data. Groups were compared using the Chi-square test for categorial variables and the Fisher exact test when necessary.

The receiver-operating-characteristic (ROC) analysis was used to obtain the area under the curve for evaluating the accuracy of SUV_{max} and its cut-off value. Sensitivity, specificity, prevalence, positive predictive value and negative predictive value were calculated.

The *P* value was considered significant when less than 0.05. Statistical analysis was performed using dedicated software (SPSS®, version 23.0; IBM®).

5 Results

5.1 Patient Characteristics

Overall, 30 patients (16 men and 14 women; median age 62 y; IQR 53-69 y) with pNETs were included in the study. Four patients (13.3%) had functioning tumours: three insulinomas and one glucagonoma. In the remaining 26 patients (86.7%), the tumour was non-functioning. According to the 2010 WHO classification, 16 patients (53.3%) had a G1 pNET, 12 (40%) a G2 pNET and one patient (3.3%) a G3 pNET. One single patient (3.3%) had a histologically proven pNET without specification of Ki-67 index and WHO Grading. In twelve patients a primary tumour was detected and in one patient a local relapse of pNET was noted. The other remaining 17 cases were part of the restaging programme.
All characteristics of the 30 patients are listed in table 5. In case of multiple lesions, we reported the highest SUV_{max} for calculating the median.

Surgery consisted of splenopancreatectomy (6 cases), standard Whipple procedure (2 cases), pylorus-preserving Whipple procedure (1 case), distal pancreatectomy (4 cases), intermediate pancreatic resection (3 cases), total pancreatectomy (1 case), and standard Whipple procedure with splenopancreatectomy (1 case). In one case metastasectomy of liver metastases was performed.
Four patients received distal pancreatectomy, and one patient splenopancreatectomy after being examined for this study.

Table 5: Clinical features of the 30 patients who underwent ^{68}Ga-DOTA-NOC PET/CT

SUV_{max} Median and IQR (25^{th}-75^{th} percentiles) among different groups of patients

[1] 5 out of the 10 patients received surgery after the examination date

[2] due to single value no Median calculable

Patient characteristic	No. of patients	SUV_{max} Median	SUV_{max} IQR
Sex			
male	16	31.94	11.67-78.96
female	14	27.60	8.13-43.48
Functioning			
yes	4	61.30	22.57-78.96
no	26	25.84	8.13-49.73
Clinical stage			
Localized	5	44.00	37.50-84.89
metastatic	15	35.71	23.50-64.24
no pathological findings	10	6.99	4.16-13.65
Treatment			
Surgery	18	14.25	5.73-56.04
Chemotherapy	1	83.45[2]	-
PRRT	1	25.38[2]	-
None[1]	10	39.51	27.77-55.51
2010 WHO classification/Ki-67 Index (%)			
G1/≤2	16	33.15	9.12-73.00
G2/3-20	12	25.84	7.48-53.90
G3/>20	1	35.65[2]	-

5.2 SUV_{max} Cut-off value of ^{68}Ga-DOTA-NOC

SUV_{max} was calculated by measuring the maximal concentration of the labelled tracer in the region of interest corrected for body weight and injected dose (SUV_{max} = maximum activity concentration/[injected dose/body weight]) [31]. For large pancreatic tumours, the region of interest (ROI) was moved over several sites within the mass to ensure that the correct SUV_{max} was obtained.

The cut-off value was received by the receiver operating characteristic analysis (SPSS®, version 23.0; IBM®) by verifying the highest accuracy (accuracy = (sensitivity + specificity)/2). In this case, it is 0.8, as shown in table 6. The identified SUV_{max} cut-off value of ^{68}Ga-DOTA-NOC in patients with neuroendocrine pancreatic tumour is 23.27 (rounded to two decimal figures).

In this study, SUV_{max} lower than 23.27 can be interpreted as physiological uptake of the pancreas. The highest non-tumorous uptake was found in the pancreatic head.

Eleven patients out of 20 (55%; G1: n=8, G2: n=2, G3: n=1), who had a histologically proven pancreatic neuroendocrine tumour, were measured with a SUV_{max} in the pancreas higher than the cut-off value and were diagnosed with a primary tumour. One patient out of 20 (5%) had a relapse with two foci in the pancreatic body, and was also measured with a SUV_{max} in the pancreas higher than the cut-off value. The other 8/20 (40%) remaining patients had values lower than the cut-off.

Going into detail, one of those eight patients had a primary tumour and metastases with histology but missing Ki-67 index and grading, which had a SUV_{max} under the cut-off value. The other seven patients (G1: n=1, G2: n=6) had no increased tracer-uptake in the pancreas but had distant lesions. In those cases, patients received pancreatic surgery before PET/CT scans were done. The maximum tracer uptake in distant metastases (lymph nodes, liver, bone) was lower than the cut-off of SUV_{max} in 3/7 of these patients (G1: n=1, G2: n=2).

All in all, the remaining 10 patients (G1: n=6, G2: n=4) of this study with non-suspicious findings (figure 4) had a SUV_{max} in the pancreas lower than the calculated cut-off value (median=6.99, IQR=4.16-13.65).

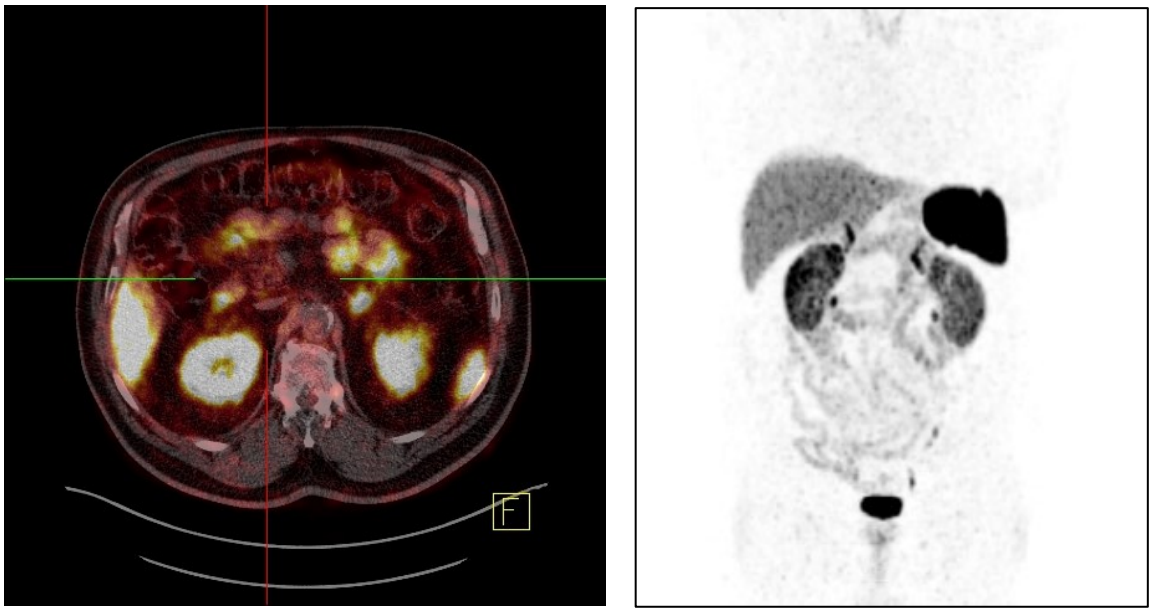

Figure 4: Non-suspicious finding with SUV_{max} 13.06 measured in the pancreas

The same region of interest with ^{68}Ga-DOTA-NOC is shown in two different types of imaging: PET/CT (left) and MIP (right)

SUV_{max} is an optimal parameter for semiquantitative analysis due to its informal assessment in a non-invasive method. It can be regarded as a whole-body procedure with PET/CT and affords functional evaluation of the whole tumour burden. This is not possible with the Ki-67 index.

Table 6: ROC Analysis chart

[1]The minimum is the lowest observed value minus 1; the maximum is the highest observed value plus 1. All other values are mean values of two consecutively ordered and observed values.

SUV_{max}[1]	Sensitivity	1- Specificity	Accuracy
2.0100	0.000	0.000	0.5
3.4700	0.100	0.000	0.55
4.0000	0.200	0.000	0.6
4.0900	0.200	0.050	0.575
4.1700	0.200	0.150	0.525
4.4150	0.300	0.150	0.575
5.3500	0.400	0.150	0.625
6.6000	0.500	0.150	0.675
7.2000	0.500	0.200	0.65
7.4300	0.500	0.250	0.625
7.7150	0.500	0.300	0.6
8.0400	0.600	0.300	0.65
9.8600	0.700	0.300	0.7
12.1300	0.700	0.350	0.675
13.9050	0.700	0.400	0.65
14.2450	0.800	0.400	0.7
18.2900	0.900	0.400	0.75
23.2650	**1.000**	**0.400**	**0.8**
28.5350	1.000	0.450	0.775
32.4200	1.000	0.500	0.75
34.4000	1.000	0.550	0.725
39.4800	1.000	0.600	0.7
43.6550	1.000	0.650	0.675
44.1450	1.000	0.700	0.65
45.9700	1.000	0.750	0.625
63.1250	1.000	0.800	0.6
78.8400	1.000	0.850	0.575
81.2650	1.000	0.900	0.55
87.3150	1.000	0.950	0.525

92.1800	1.000	1.000	0.5

All summarised data result in the blue line (ROC curve) and are interrelated to the green diagonal (figure 5). The farthest intersection in relation to the diagonal shows the highest accuracy, which leads to the correct cut-off value 23.27 with the optimal sensitivity and specificity.

In this case, (1-specificity) was used to avoid a resulting descending curve. Therefore, the x-axis goes from 0 to 100% instead of 100 to 0% (specificity).

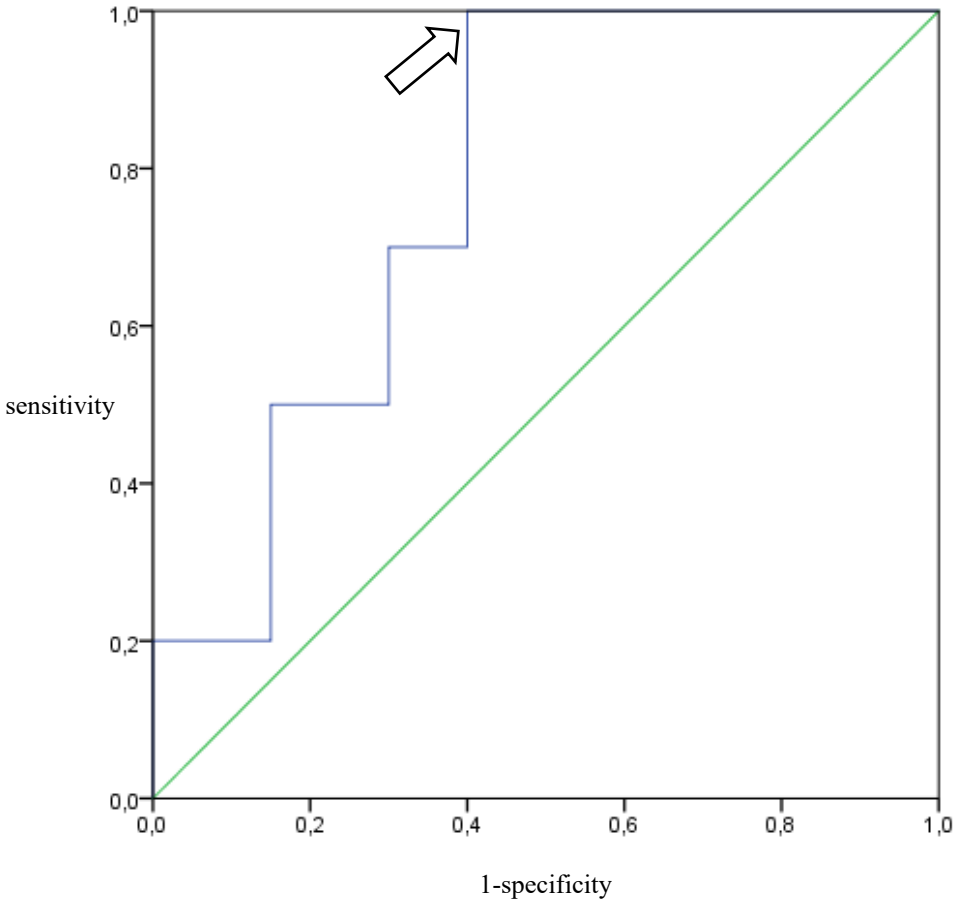

Figure 5: ROC curve for SUV_{max}

The arrow displays the point of intersection at a specificity of 60% (1-0.4) and a sensitivity of 100%.

5.3 Patient-based Analysis

Twenty patients out of the 30 with histologically proven pNET had pathological ^{68}Ga-DOTA-NOC metabolised lesions in the pancreas with or without metastases. This manifests

a prevalence (= (affected patients with histologically proven pNET/ all patients) x 100) of 67%.

Based on histopathological findings and multiple follow-ups, the patient-based sensitivity, specificity, and diagnostic accuracy were each 100% since there were no false positive and false negative cases.

The positive predictive value (= [sensitivity x prevalence] / [sensitivity x prevalence + (1-specificity) x (1- prevalence)]) of this study is 1 and the negative predictive value (= specificity x (1- prevalence) / [(specificity x (1-prevalence) + (1-sensitivity) x prevalence)] is 1.

The most common site of origin of the primary tumour within the pancreas (n=12) was the tail (7/12, 58%), followed by the body (3/12, 25%) and the head (2/12, 17%); in one case, there were multiple foci of a neuroendocrine tumour within the pancreas.

Table 7: Clinical features of the 20 patients with suspicious finding according to SUV_{max}

Categorial variables are expressed as n (%) and evaluated using Chi-square test.

Patient characteristic	No. of patients	SUV_{max} Median	SUV_{max} IQR	*P*
Sex				
male	11(55)	64.24	28.17-91.18	<0.0001
female	9(45)	35.65	27.60-45.83	
Functioning				
yes	3(15)	78.60	44.00-79.08	0.001
no	17(85)	35.71	25.84-60.23	
Ki-67				
≤5%	11(55)	44.00	34.60-79.08	<0.0001
>5%	8(40)	41.65	24.67-62.18	
2010 WHO classification				
G1	10(50)	50.11	33.87-82.11	<0.0001
G2	8(40)	41.68	24.67-62.18	
G3	1	35.65	-	

As reported in table 7, there were significant differences with respect to sex, functioning, Ki-67 index, and 2010 WHO classification. SUV_{max} was significantly higher (P<0.0001) in male patients (n=11; median 64.24; IQR 28.17-91.18) than in females (n=9; median 35.65; IQR 27.60-45.83). There was also a significance in terms of functioning (P=0.001), Ki-67 (P<0.0001), and 2010 WHO classification (P<0.0001).

5.4 Lesion-based Analysis

Pancreatic tracer uptake over the above determined cut-off value was detected in twelve cases. In one case with a proven pNET and absent histological classification, the uptake was lower than the cut-off value and the patient`s restaging showed a primary tumour.

As above mentioned, twelve patients had a primary tumour, including one patient showing an additional pancreatic metastasis in the tail. A relapse with 2 foci in the pancreatic body was detected. The characteristics of all 13 patients who showed a pathological ^{68}Ga-DOTA-NOC-uptake are summarised in table 8.

Table 8: Overview of all pancreatic lesions

[1]volume = (cm^3)

Pancreas	No. of lesions	SUV_{max} Median	SUV_{max} IQR	Volume[1] Median	Volume IQR
Primary					
caput	2	51.99	-	17.55	-
corpus	3	35.65	-	26.57	-
cauda	7	44.00	31.69-83.45	17.68	5.33-30.86
local recurrence	2	34.19	-	11.25	-
metastasis	1	11.41	-	4.54	-
Total	15	43.31	25.38-78.6	17.68	5.67-27.88

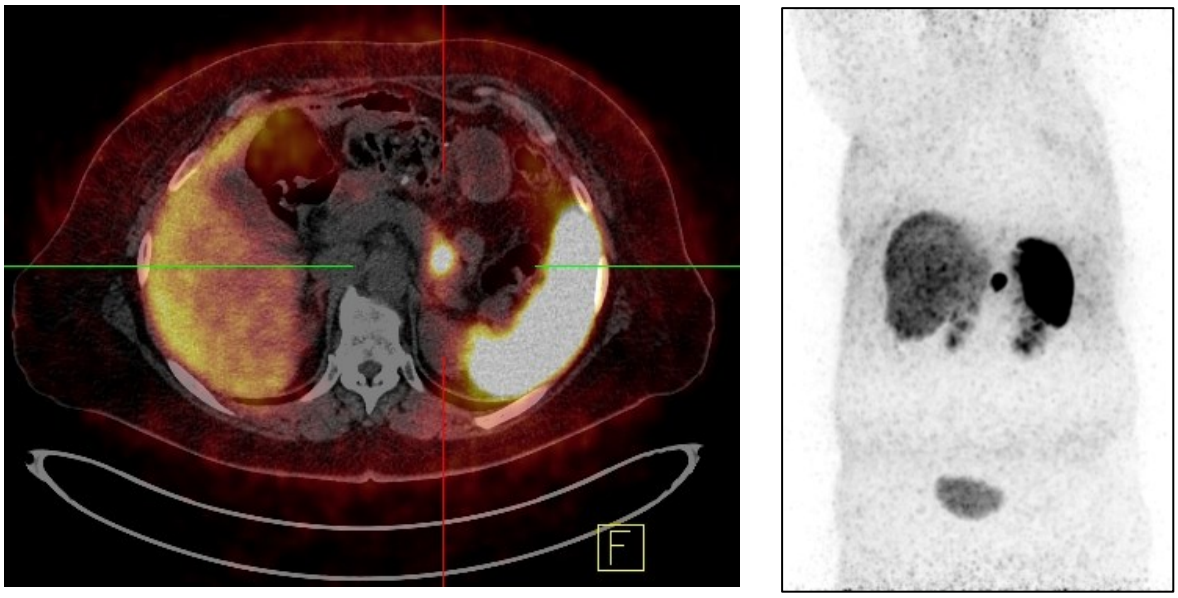

Figure 6: Primary identified in the pancreatic cauda with SUV_{max} 44.00 and volume of 31.49 cm^3
The same lesion with ^{68}Ga-DOTA-NOC is shown in two different types of imaging: PET/CT (left) and left lateral MIP (right)

^{68}Ga-DOTA-NOC SUV_{max} was measured in 253 extrapancreatic lesions, all considered as distant metastases and in one locoregional metastasis in the pancreatic tail. Most metastases were detected in the liver (n=217, median SUV_{max} 83.24, IQR 24.43-60.23) in 13 patients, followed by lymph nodes (n=18, median SUV_{max} 30.74, IQR 11.61-110.33) in 3 patients, bones (n=14, median SUV_{max} 5.37, IQR 1.95-8.78) in 3 patients, and lungs (n=3, median SUV_{max} 13.57) within one patient. One metastasis in the rectum was detected (median SUV_{max} 34.6).

All in all, 14 patients (14/20, 70%) had metastases outside the pancreas. The other six patients (6/20, 30%) presented with pathological uptake only in the pancreas. Three patients (3/20, 15%) had more than one location of metastases; two patients (2/20, 10%) even more than two.

The estimated quantity of metastases in organs with uncountable foci for the human eye was defined to be 20.

The highest median volume (table 8) was measured in the pancreatic body, followed by the tail and the head. Pancreatic metastases were of small volume in this study. In one case, there was a local relapsed status of tumour disease with 2 foci which had a median volume lower than in primary tumours but higher than pancreatic metastases.

The lesion-based sensitivity, specificity, and diagnostic accuracy for 15 pancreatic lesions and 253 distant metastases were 100%, respectively.

Table 9: Overview of all distant metastases

Tumour *yes* indicates a pathological finding. Ten patients showed no significant pathological uptake in the pancreas.

Patient	**Tumour**	Liver	Lnn.	Lung	Rectum	Bone	**Sum of metastases/ patient**
1	Yes						0
2	Yes						0
3	Yes	20					20
4	No						-
5	No						-
6	No						-
7	Yes	20					20
8	No						-
9	No						-
10	Yes	20		3	1		24
11	Yes	9					9
12	Yes	20	10				30
13	No						-
14	No						-
15	Yes		2				2
16	No						-
17	Yes						0
18	Yes	20					20
19	Yes	20					20
20	Yes						0
21	No						-
22	Yes	3					3
23	Yes	20					20
24	Yes	20				1	21
25	Yes	5					5
26	Yes	20				12	32
27	No						-
28	Yes						0
29	Yes	20	6			1	27

30	No						-
Total		***217***	***18***	***3***	***1***	***14***	***253***

253 lesions could be detected as distant metastases (table 9). All of them had a histological result of proven metastases of the pNET but only a few of them with the indication of tumour grading. Twenty lesions in the liver were G1 differentiated (20/217, 9.22%), 52 were G2 (52/217, 23.96%), and 40 were G3 (40/217, 18.43%). Two lymph node metastases were G2 differentiated (2/18, 11.1%), and the only rectal metastasis was G1 differentiated (100%).

5.5 Somatostatin Receptor Scintigraphy (SRS)

SRS is nowadays routinely used as the main imaging method for NETs after a period of establishment for over 20 years. In many cases, it shows high diagnostic accuracy in imaging the whole body where CT cannot identify the primary lesion. Some limitations were reported: lack of receptor expression, difficulty identifying small lesions (< 10 mm), unsuspected lesions in small size, and evaluating tumours in organs with high physiological uptake (e.g. pancreas or liver) [19] [15] [32]. SRS with CT (SPECT) is indicated in cases where metastases should be detected. Several authors report a sensitivity of SRS between 61-96% [15]. An additional limitation is the poor anatomic resolution compared to PET/CT [33].

5.5.1 ^{111}In-Octreotide Scintigraphy

A common method of nuclear medicine for diagnosing neuroendocrine tumours of the gastroenteropancreatic system is the use of octreotide, a somatostatin analogon. With its short half-life of fewer than 2 minutes, the development of analogues was necessary. Pentetreotide, a conjugate of octreotide, binds to SSR-2 and SSR-5.

The sensitivity for functioning NETs is described as 75-100% in several studies, except for insulinoma with a sensitivity of less than 50-60%. Physiological uptake can be seen in the hypophysis, liver, spleen, thyroid, and the kidneys. Due to the relatively long half-life period of ^{111}In of 2.8 days, imaging can begin only 4 hours post injection. Best image quality is obtained after 24 hours post injection. For adults, the optimum dose is 10 to 20 µg with 222 MBq of activity with proven non-pharmacological effect. Indications for scintigraphy are staging of NETs, identifying somatostatin receptors on tumour cells to evaluate the possible effectiveness of octreotide therapy, and detecting any relapse [34] [35] [36] [37].

^{111}In-pentetreotide displays a lower affinity to SSR-2 than ^{68}Ga-DOTA-peptides do: the half-maximal inhibitory concentration is 22 nM for ^{111}In-pentetreotide, compared to 1.9 nM for ^{68}Ga-DOTA-NOC [4].

In a retrospective study, the pancreatic to hepatic uptake ratio was calculated to distinguish between physiological and pathological tracer uptake in patients with pancreatic NETs. This study also confirmed that the most physiological uptake could be found in the uncinate process (ratio below 2). One disadvantage was the doubled interpretation of SPECT/CT images (6 and 30 hours post injection) to specify the exact location, shape, and intensity of the lesion [38].

There are several deficiencies of ^{111}In-pentetreotide SPECT imaging in clinical use compared to ^{68}Ga-DOTA-peptide PET imaging: non-detection of smaller lesions, assured detection of lesions with only high SSR expression, detection of fewer lesions, slower imaging procedure, higher exposure of radiation, and non-detection of occult primary tumours of patients with previous negative results on conventional imaging [4].

5.5.2 ^{99m}Tc-HYNIC-TOC

Besides ^{111}Indium-linked pentetreotide, HYNIC-TOC (Tyr3-octreotide) attached to ^{99m}Technetium is used in clinical routine for diagnosis, staging, and restaging programme of NETs. Excellent physical characteristics are gamma rays with 140 keV, half-life of 6 hours, higher available activities (in adults: 350-925 MBq), and less radiation exposure. The synthesis of ^{99m}Tc-octreotide is cheaper than of ^{111}In since no cyclotron for production is necessary and the radionuclide can be extracted from a commercial generator [35] [39].

A study of 30 patients with NETs, mostly with tumours of the gastroenteropancreatic system, showed a sensitivity of 87% and a specificity of 86%, using ^{99m}Tc-HYNIC-TOC scintigraphy [40].

A Hungarian study investigated the pitfalls and benefits of this tracer. Higher tumour/background ratios are found in ^{99m}Tc-HYNIC-TOC compared to ^{111}In-tracers. Improved diagnostic accuracy is reached over higher resolution resulting in better registration on SPECT/CT. Lesion localisation is worse in ^{111}In-octreotide images. SRS shows lower sensitivity in lesions which occur in organs with high physiological tracer uptake, such as the liver or pancreas. Several cases were reported with high uptake of ^{99m}Tc-HYNIC-TOC in benign lesions due to overexpression of SSR (e.g. degenerative bone disease, fractures, inflammatory processes, and epiphyseal growth plates). SSR expression

was also found in other pathological cases, such as meningioma or breast cancer. This leads to incidental findings during NET imaging examination. Higher energy of the emitted rays and longer half-life occur in ^{111}In. These are the reasons why ^{99m}Tc-HYNIC-TOC was selected to be the best option for SPECT imaging. The pharmacokinetic characteristics of it are superior to ^{111}In-octreotide, and higher values of tumour tracer uptake were measured [41].

Hou et al. described SPECT and planar scintigraphy as the most popular imaging method in nuclear medicine. Therefore, ^{99m}Tc-HYNIC-TOC is suitable due to easy accessibility (single-vial kit formulation) and fewer costs [39].

Liepe et al. described the lower sensitivity of ^{99m}Tc-HYNIC-TOC in detecting primary NET compared to follow-ups (67% vs. 92%). There was one false-positive and three true-positive findings within the pancreas. A slightly higher sensitivity of ^{99m}Tc-HYNIC-TOC is given in comparison to ^{111}In-octreotide. The use as an optimum radiotracer for tumours with SSR expression when ^{68}Ga-DOTA-peptides are not available is indicated. Due to the possibility of image acquisition up to 4 hours post injection, the exclusion of physiological tracer uptake is possible [42].

5.6 Positron emission tomography with radiopharmaceuticals

5.6.1 ^{18}F-FDOPA

The blood-brain barrier can be crossed by L-DOPA. This fact had led to the creation of ^{18}F-FDOPA (6-[18F]Fluoro-L-3,4-dihydroxyphenylalanin) in the 1980s as a PET-tracer. The fluorinated analogon of L-DOPA illustrates the dopamine metabolism in the human brain. Higher activity of decarboxylase can be found in NETs which also accumulate L-DOPA. With this imaging method, benign and malignant, or functioning and non-functioning tumours, can be distinguished. NET cells proportionally take up ^{18}F-DOPA to their cell metabolism. Highly proliferating undifferentiated pNETs can be visualised [19] [43] [44]. Unexpected tracer uptake can occur in inflammatory pancreatic lesions and should be kept in mind, such as diffuse physiological uptake in gallbladder and pancreas. Compared to somatostatin analogues or FDG, which are easier absorbed by leucocytes, FDOPA is more tumour specific [32].

The physical half-life of ^{18}F-FDOPA is 109.7 minutes. For application, the optimum pH-value should be about 5 for the human body. Therefore, sodium bicarbonate must be added

as a buffer. The patient`s radiation exposure is 6 mSv [43], a lower dose delivered to organs than in patients with ^{68}Ga-DOTA-NOC PET/CT [19].

NETs can absorb, decarboxylate, and store amino acids (e.g. DOPA), and their biogenic amines [32].

A study with 24 patients with abdominal carcinoid tumours and proven high serotonin metabolism confirmed the superior sensitivity of FDOPA PET/CT in terms of per-lesion analysis with a sensitivity of 80% and could outmatch SRS. The use of FDOPA PET/CT in imaging patients with digestive NET can be regarded as the first-line functional imaging modality [45].

FDOPA PET/CT has good results in children with focal hyperplasia of beta cells in the pancreas. A German study by Mohnike et al. confirmed this: all lesions were detected and could be successfully excised. Complete healing was achieved in 87-91% of the operated cases [46]. FDOPA PET possesses the ability to distinguish between focal and diffuse congenital hyperinsulinism and facilitates pancreatic surgical intervention by guiding [32].

Schiesser et al. showed in a prospective study with 61 patients who underwent FDOPA PET/CT and SRS a sensitivity of 91% and a specificity of 96% for FDOPA, whereas SRS demonstrated only 59% and 86%, respectively [47].

SRS, CT or both methods combined detect fewer lesions in metastatic NETs than ^{18}F-DOPA with a sensitivity of nearly 100% [15]. It is superior in patients with low-grade NETs in terms of detecting lymph nodes, bone lesions, and liver metastases [19]. In high-grade gastroenteropancreatic NETs, ^{18}F-FDOPA PET/CT has a moderate sensitivity of 25% but is more useful in carcinoids where high activity of aromatic L-amino acid decarboxylase can be found. This enzyme is part of the biosynthesis of serotonin within the tumour [4].

In cases with metastatic tumour disease, FDOPA precisely detected bone lesions (100% of sensitivity), even in 40% of cases with previous negative CT scan [32].

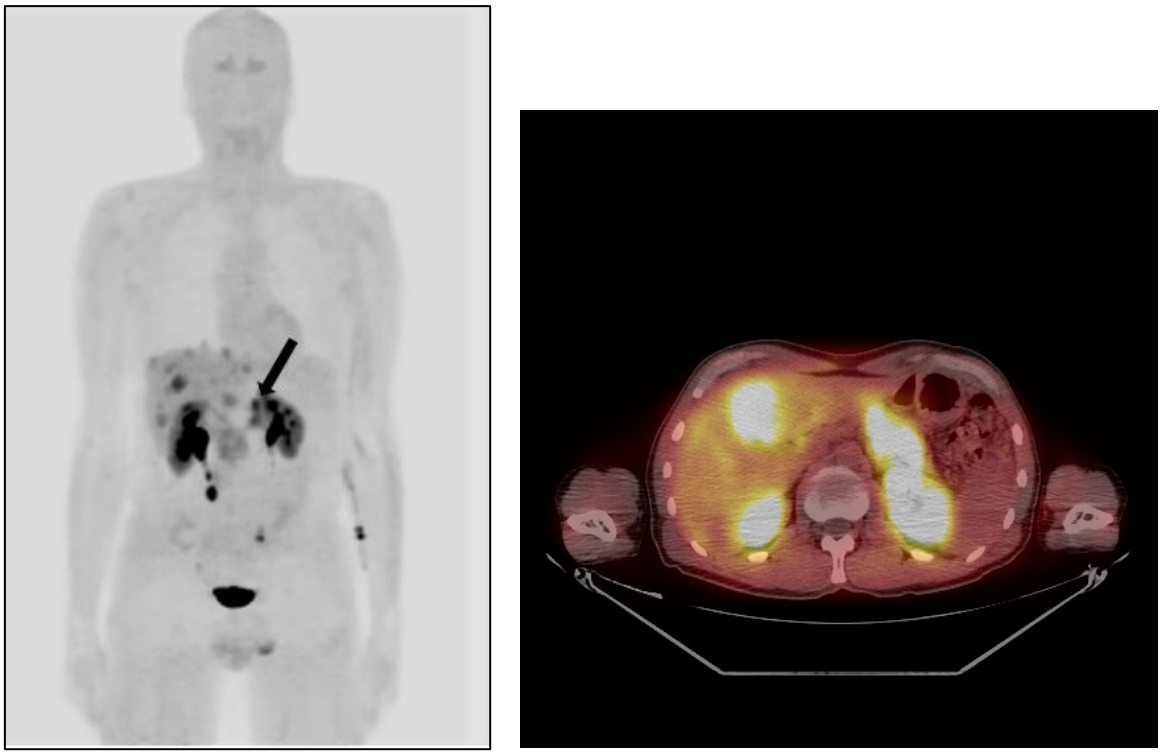

Figure 7: ^{18}F-DOPA PET/CT MIP and axial PET/CT of the same patient
A primary pNET in the pancreatic tail (arrow) and liver metastases were detected.

Hoegerle et al. described that 84% of all false-negative ^{18}F-DOPA findings (35%) occurred in tumours with no serotonin expression. In serotonin-expressing carcinoids, ^{18}F-DOPA can distinguish between small benign and malignant lymph nodes (< 10mm), and localise the primary tumour. All in all, ^{18}F-DOPA PET had a sensitivity of 65% in this study and was only inferior to morphologic procedures (computed tomography and/or magnetic resonance imaging) with a sensitivity of 73%. Optimum results were obtained with a combination of the mentioned imaging methods [33].

5.6.2 ^{18}F-FDG

^{18}F-FDG, the most used tracer, has a half-life of 109.7 minutes and contains cyclotron-synthesised ^{18}F as radionuclide and a glucose analogon. FDG is absorbed like glucose in the human body and accumulates in regions with high demand for glucose. In tumours, the same behaviour can be found: over-expression of glucose transporters and elevated activity of hexokinase lead to metabolic trapping. Tumour cells are not able to export phosphorylated FDG, which increases the intracellular accumulation of FDG [34] [48] [49].

^{18}F-FDG PET/CT is used to distinguish benign and malignant lesions, for paraneoplastic syndrome, to detect primaries and/or metastases in cases with primary of unknown origin, for staging, to detect relapse status, and to plan radiation therapy [48].
Several guidelines must be observed to minimise artefacts. Non-diabetic patients are not allowed to eat or drink sweet liquids/alcohol at least 4 hours before imaging. The optimum blood sugar level would be 4 to 7 mmol/l. During tracer-injection and examination time, patients are not allowed to move. Otherwise, the result would be biased by elevated FDG-uptake in muscle cells. The urinary bladder should be empty at the time of examination.
Tracer activities are weight-dependant. Usually, activities between 300 to 400 MBq are clinical routine, twice as much as with ^{68}Ga-DOTA-NOC. Examination time is identical with the used tracer in this study: 60 minutes post injection. Artefacts using ^{18}F-FDG as tracer are caused by moving patients while acquiring images, and with patients on metformin therapy. This is reflected in higher gastrointestinal tracer uptake [48] [50].
A prospective study in 87 patients (38 male, 49 female, median age 46.0 y) with von Hippel-Lindau disease and solid pancreatic NETs compared ^{18}F-FDOPA, ^{18}F-FDG PET, CT, and MRI. All patients received pre-treatment with 200 mg Carbidopa one hour before injection. SUV_{max} values were measured of pancreatic and extrapancreatic lesions. Only 11 of 98 pNETs detected by CT (11% of the total amount of detected lesions) were identified in ^{18}F-FDOPA PET and 45 of 98 (46%) in ^{18}F-FDG PET. The conclusion of this study was the minor value of ^{18}F-FDOPA PET in diagnosing pNETs. ^{18}F-FDG PET on its own was not able to detect all lesions; in combination with CT better rates of detection could be reached [51].

It has been reported that neuroendocrine tumours with undifferentiated histological status and primary bronchial NETs are better identified by ^{18}F-FDG, which is more accessible than ^{18}F-DOPA [15] [52]. Many authors reported that ^{18}F-FDG PET could be more suitable for patients with G3 NETs [8] [53] and in some cases for high-grade G2 tumours [4] with little or absent hormone production [32]. For the possible use of ^{18}F-FDG PET/CT in patients with well-differentiated NETs (G2), the Ki-67 index should be at least 10% [4]. In the present study, well differentiated pNETs were successfully detected with the use of ^{68}Ga-DOTA-NOC PET/CT (figure 8).

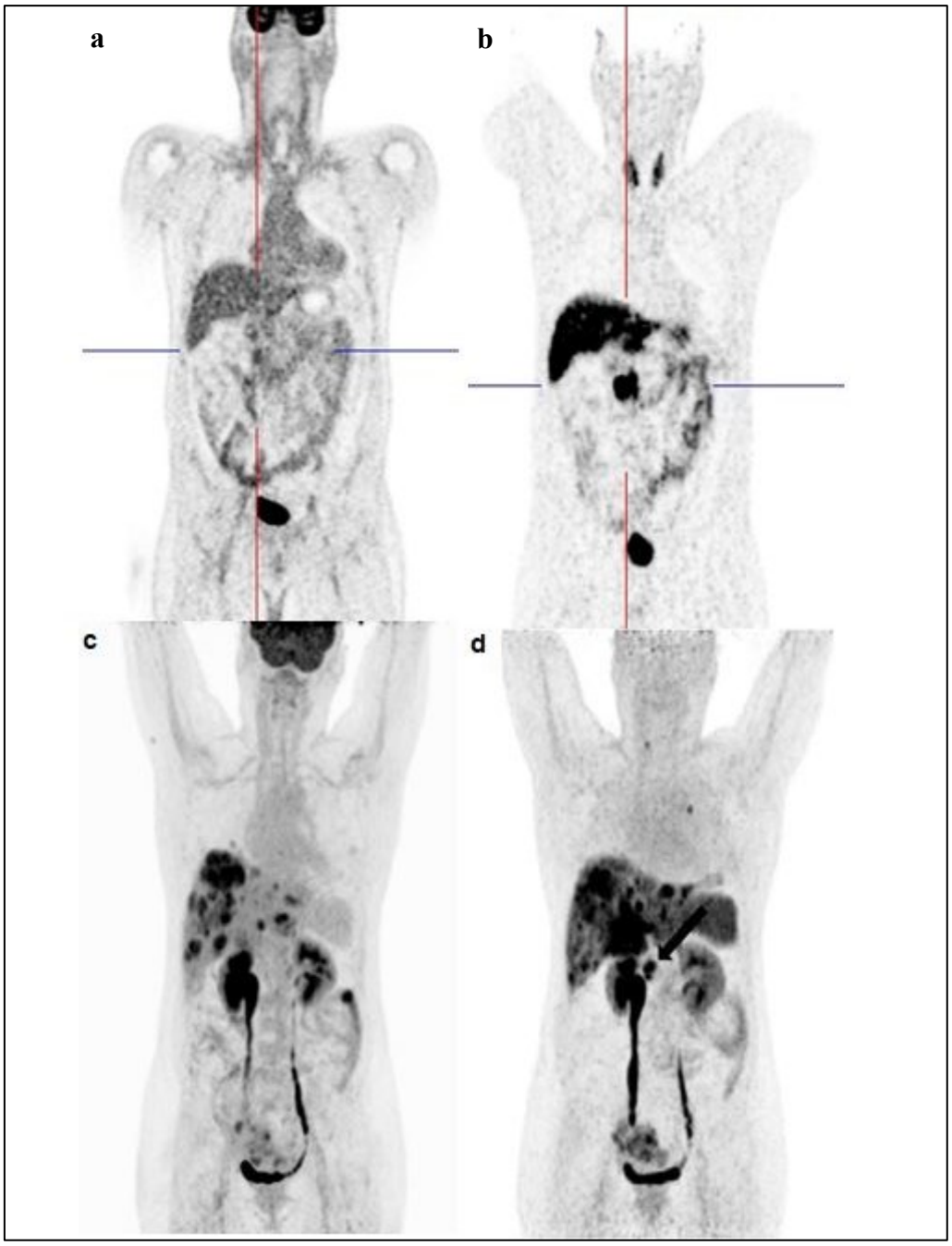

Figure 8: Comparison of ^{18}F-FDG and ^{68}Ga-DOTA-NOC in MIP of PET/CT within the same two patients

Both patients had histologically proven pNET G1. One patient had significantly more tracer uptake in the pancreatic head in ^{68}Ga-DOTA-NOC PET/CT (b) compared to the prior examination with ^{18}F-FDG (a). The other patient (d) showed pathological tracer uptake in the pancreas with ^{68}Ga-DOTA-NOC PET/CT alone, resulting to be a primary in the head of the pancreas (arrow). ^{18}F-FDG showed only increased tracer uptake in the liver metastases but no significant tracer uptake in the pancreas (c).

In a study with 18 patients, 15 were suffering from foregut NET, FDG patient-based sensitivity was 100% vs. 83% for SRS, and FDG PET detected more lesions than SRS in 78% of cases [54].

In the study of Cingarlini et al. analysing the role of combined ^{68}Ga-DOTA-TOC and ^{18}F-FDG PET/CT in the diagnostic workup of pancreas neuroendocrine tumours in 35 patients, the tumour grade significantly correlated with ^{18}F-FDG uptake (P = 0.002 with Ki-67 cut-off 2-20% and P = 0.009 with Ki-67 cut-off 5-20%). Detecting G2 lesions showed a high positive predictive value (90.5%). ^{18}F-FDG PET/CT was positive in more G2 tumours compared to G1, with an overall sensitivity of 60%. ^{68}Ga-DOTA-TOC PET/CT, however, offered high sensitivity (94%) in both groups with no significant differences [8].

6 Discussion

Based on the histopathological findings and multiple follow-ups, the patient-based sensitivity, specificity, and diagnostic accuracy for ^{68}Ga-DOTA-NOC PET/CT in the present study were each 100%. The lesion-based sensitivity, specificity and diagnostic accuracy for 15 pancreatic lesions and 253 distant metastases were 100%, respectively.

^{68}Ga, a radionuclide for PET/CT scans, has been established as the gold standard for NETs [4]. In clinical use, there are several peptides linked to ^{68}Ga: ^{68}Ga-DOTA-TOC, ^{68}Ga-DOTA-NOC, and ^{68}Ga-DOTA-TATE. DOTA, a chelator, is the linker between ^{68}Ga and the used peptide. All peptides tend to have a high affinity to SSR-2 and stronger affinity than ^{111}In-pentetreotide in SRS. Several studies report a rate of detection in SRS between 50 to 100%. PET/CT, in combination with ^{68}Ga-DOTA-peptides, enables the identification of smaller NETs with less frequency of SSR on the tumour cell surface [34] [4] [20]. A combination of ^{68}Ga-DOTA-peptide PET with an optimised multiphase CT can improve the management of a patient [4]. A prospective American study by Sadowski et al. showed that ^{68}Ga-DOTA-TATE PET/CT detected 95.1% of all gastroenteropancreatic lesions, whereas anatomic imaging (45.3%) and ^{111}In-pentetreotide SPECT/CT (30.9%) provided worse results [55]. Sensitivities between 87 to 96% were reported for ^{68}Ga-DOTA-TOC PET [15] [8]. A Hungarian study also confirmed that ^{68}Ga labelled peptides result in higher resolution using PET as image modality for patients with NETs and have lower radiation exposure [56].

^{68}Ga-DOTA peptides also provide additional information on receptor status, which is required before starting targeted radionuclide therapy. Their mechanism of binding to somatostatin receptors on the cell surface is helpful to rate the pNETs in terms of cell differentiation indirectly. A high receptor expression can be found in well-differentiated NETs [19]. The benefit of ^{68}Ga-DOTA-NOC is the additional affinity to SSR-3 [20].
In the study of Ambrosini et al., ^{68}Ga-DOTA-NOC detected more lesions compared to ^{18}F-DOPA (71 vs. 45), notably in the liver, lung, and lymph nodes. Furthermore, more primary tumours were correctly identified (6 vs. 2). In eight locoregional lesions, only ^{68}Ga-DOTA-NOC could state the malignancy, while DOPA was negative. Regarding all lesions, SUV_{max} of ^{68}Ga-DOTA-NOC was higher in each lesion [19].

To identify an unknown primary and/or assessing secondaries ^{68}Ga PET/CT is the first choice due to its high sensitivity [15].

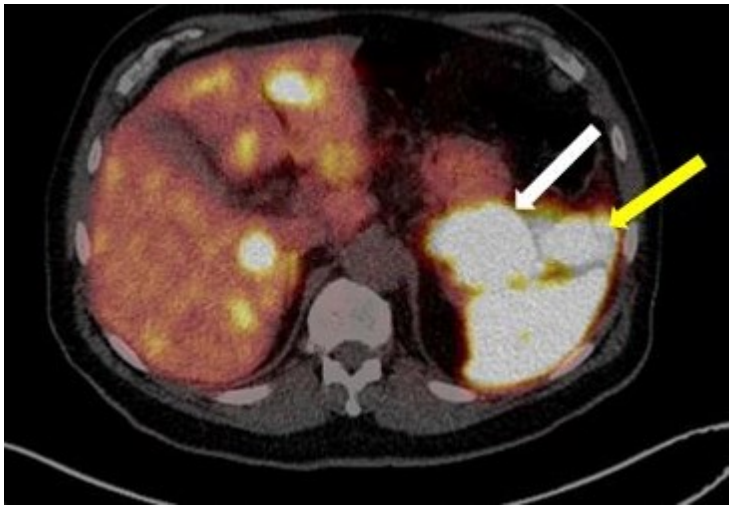

Figure 9:Detection of pancreatic primary and metastases with ^{68}Ga-DOTA-NOC PET/CT
Pancreatic NET in the tail (white arrow) and lymph nodes with pathological tracer uptake (yellow arrow) as well as liver metastases were identified.

^{68}Ga-DOTA-NOC PET/CT also had an impact on either staging or treatment change in 50 of 90 patients (56%) with pNET in a reported study [57].
As mentioned earlier, SRS imaging is not suitable due to its low sensitivity for insulinoma detection. Recent studies show that ^{68}Ga-peptide PET can identify benign and malignant insulinomas in more than 85% of all cases [4]. The team of Antwi et al. started a pilot study to verify the effect of ^{68}Ga-DOTA-exendin-4 PET/CT to localise occult insulinomas. ^{68}Ga-DOTA-exendin holds the GLP-1 receptor as a target [58]. In literature several pitfalls of interpreting SRS PET are listed: physiological uptake in the pancreatic head and uncinate process, accessory or intrapancreatic spleen, splenosis as metastases of pNET, and misinterpreting inflammatory uptake as tumour disease (e.g. inflammation in lymph nodes or joints) [4].

Ambrosini et al. confirmed the result of the present study of accuracy using ^{68}Ga-DOTA-NOC in patients with suspicion of neuroendocrine tumour (98% vs. 100%) even though the method was not recommended as a first-line imaging technique in patients with increased blood markers alone [59].

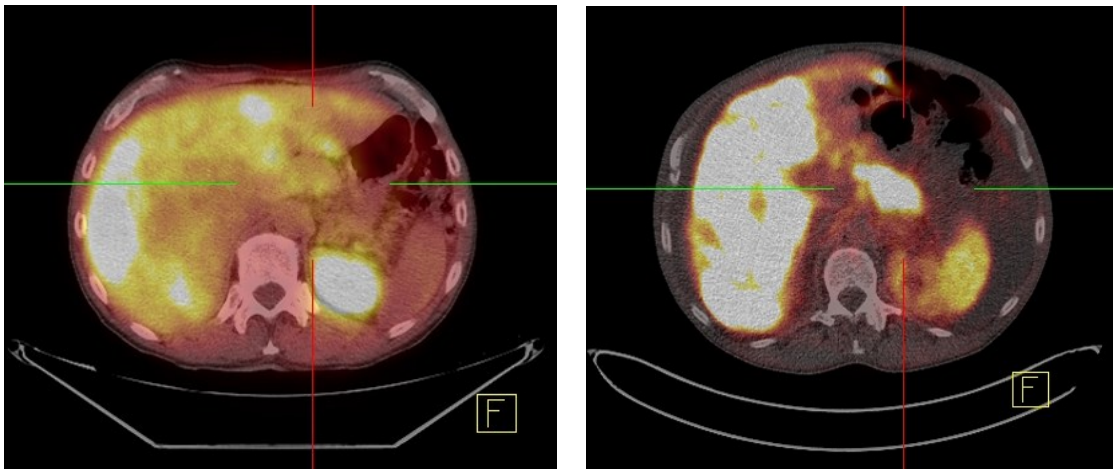

Figure 10: ^{18}F-DOPA (left) and ^{68}Ga-DOTA-NOC (right) PET/CT images of the same patient
In both images, the region of interest is shown by the crosslines. Significantly higher tracer uptake can be measured in the pancreatic body with ^{68}Ga-DOTA-NOC, which led to the detection of the primary tumour.

A 2010-published prospective study of 47 patients (27 male, 20 female, median age 62.8 y) with histologically proven NET investigated ^{68}Ga-DOTA-NOC PET scans as a non-invasive marker for prognostic issues of NETs. The region of interest, as in our study, was chosen with the highest tracer uptake. 23 patients (48.9%) had a pancreatic neuroendocrine tumour, and 42 patients (89.4%) had a well-differentiated neuroendocrine carcinoma. The SUV_{max} of patients with pNET was significantly higher than in gastrointestinal NETs or NETs of the lung. No differences between SUV_{max} in terms of functioning were identified. There was significant higher tracer uptake in well-differentiated NETs compared to undifferentiated. Due to the significant results, ^{68}Ga-DOTA-NOC is seen as a useful prognostic tool for pNETs [60].

As above explained, ^{68}Ga-DOTA-peptides are the suitable tracer for pNETs with high SSR-expression to detect a primary, possible metastases, for restaging, and control the effectiveness of SSR-mediated radionuclide therapy. Special attention must be paid to NETs in the pancreas: the pancreatic head with its high frequency of SSR-2 in the islets can mimic focal tumour disease [20].

The article by Wild et al. in 2013 included 18 patients with gastroenteropancreatic neuroendocrine tumour. ^{68}Ga-DOTA-NOC PET detected 232 of 248 lesions (sensitivity 93.5%) resulting from being superior compared to ^{68}Ga-DOTA-TATE PET where only 212 lesions could be identified (sensitivity 85.5%). The main difference between these two tracers was the detection rate of metastases: ^{68}Ga-DOTA-NOC had a higher detection rate of liver metastases ($P < 0.001$), whereas ^{68}Ga-DOTA-TATE was able to detect more bone

lesions possibly explainable by the lower background activity. The specific somatostatin receptor binding profile of ^{68}Ga-DOTA-NOC might be the reason for the higher detection rate of liver metastases. Pancreatic NETs were successfully detected by ^{68}Ga-DOTA-NOC, especially in patients with MEN1 disease (87.5%) compared to ^{68}Ga-DOTA-TATE (37.5%). The significantly higher uptake of ^{68}Ga-DOTA-TATE in normal pancreatic tissue is likely responsible for the lower tumour detection rate. In two patients, both tracers showed a false-positive result in the uncinate process, which was not confirmed by other follow-ups [61]. This is a good example of how important a significant cut-off value is to distinguish between physiological and pathological tracer uptake.

Higher sensitivity of ^{68}Ga-DOTA-NOC was found in patients with G1 NETs. In three cases, therapeutic management had to be adapted to the result of the nuclear imaging with ^{68}Ga-DOTA-NOC. It showed more ample disease than other ^{68}Ga-DOTA-peptides and morphologic imaging [61].

In this study, we could also verify that tracer uptake of ^{68}Ga-DOTA-NOC indirectly correlates with tumour grade: the median SUV_{max} decreased as the tumour grade increased. There was a significant difference in the median SUV_{max} between G1, G2, and G3 pNETs ($p<0.0001$). During the process of tumour differentiation, the density of somatostatin receptors declines [61].

Although in our study there was only one patient with G3 pNET, its median SUV_{max} was significantly lower than the median SUV_{max} of G1 and G2 pNETs (table 7).

In the study of Ambrosini et al., a better outcome of pNETs was observed in patients with higher SUV_{max} [3].

Studies demonstrated the value of ^{68}Ga-peptide PET/CT in patients with previous undetected neuroendocrine tumour of unknown primary. It has a higher sensitivity and accuracy (94.0%; 63.0%) than contrast-enhanced CT (63.0%; 68.0%). Also diagnosing a relapse of NET can be performed with ^{68}Ga-peptides PET/CT with high sensitivity (90.0%) and accuracy (82.0%) [4].

^{18}F-FDOPA has a complicated synthesis process: one of the most expensive radiopharmaceuticals,^{18}F-gas, is necessary instead of ^{18}F-fluoride ions. Another limitation is the high physiological uptake in the adrenal glands, the urinary bladder, and the pancreatic head with its peripancreatic area. Image evaluation can be massively impaired by this fact [32] [62].

^{68}Ga-DOTA peptides can be synthesised much more easily than ^{18}F-DOPA. As above described, ^{68}Ga is eluted from a commercially available generator [19].
Another limitation of ^{18}F-FDOPA PET scans is the controversial pre-medication with carbidopa, an inhibitor of DOPA decarboxylase, before imaging. Some authors report higher DOPA uptake by NET cells with pre-treatment and fewer artefacts in the peripancreatic tissues since ^{18}F-FDOPA shows high uptake in the mature exocrine pancreas [19] [15]. An early image scan (5 minutes post injection) and pre-treatment with carbidopa might lead to the possible detection of insulinoma in adults [63].
Other studies reported that pre-treatment with carbidopa masks positive findings in patients with pancreatic tumours [32].

FDOPA PET/CT has a role in monitoring initial radiotherapy. Comparing images of FDOPA PET/CT, MIBG SPECT or SSR PET tumours only taking up FDOPA are less likely to respond to the planned radiotherapy or have resisted to one already carried out, while receptor-bearing NETs could have responded. This leads to false-negative results when monitoring with SSR PET [32].

Limitations of ^{18}F-DOPA are detecting small pancreatic and duodenal lesions where ^{68}Ga-DOTA-peptide PET/CT shows higher sensitivity. The only exclusion is insulinoma (pancreatic islet cell tumour), which can have low levels of SSR on its cell surface [4] [32]. This is reflected by several reported studies which show low sensitivities of SRS in insulinomas [32]. On the other hand, as Ambrosini et al. demonstrated, ^{68}Ga-DOTA-NOC had a higher per-patient detection rate than FDOPA in endocrine pancreatic tumours [19].

In the last few years, a new method for characterising tumour disease biologically was discussed. Double-tracer imaging with ^{68}Ga-DOTA-peptide and ^{18}F-FDG is the potential solution. When to perform this examination and what kind of patients would benefit from it, cannot be answered yet. Only the presence of at least one positive ^{18}F-FDG lesion minimises the prognosis for pNET [3]. These lesions tend to be more aggressive and less likely to long-term survival. The higher glycolytic rate indicates with evidence a worse prognosis to the patient. Therefore, ^{18}F-FDG PET/CT is used in patients with a metastatic NET disease [4]. In neuroendocrine tumours with no pre-treatment, ^{18}F-FDG positivity correlated with earlier tumour progression (within 6 months; $P < 0.001$) and with a significantly higher risk of exitus [8].

Pancreatic neuroendocrine tumours can be found in rare cases. The real clinical incidence is still unknown. In hospital routine, 0.5-1 out of 100.000 cases is reported. This fact leads to a humble number of potential patients for this study. The main limitation of our study was the small sample size of 30 patients. NETs of the pancreas mostly show a non-progressive course of disease what can result in a non-detection at life time. They appear in 1 % of autopsies [3] [8].

Another limitation of this study was that the diagnostic imaging procedure was performed only after the initial surgery in some patients.
A histologically proven neuroendocrine tumour of the pancreas is one of the study criteria. One of the patients with a primary had a histological result of pNET but with no further details regarding Ki-67 index and/or grading. A clearer specification of the histological result could have intensified our findings for primary lesions: patients with a ^{68}Ga-DOTA-NOC SUV_{max} under the cut-off value in the pancreas tend to have worse differentiated tumours (G2 or G3). Furthermore, in this study, only one patient had G3 pNET. Bigger sample size could have shown a more significant result for this group.

7 Conclusion

Neuroendocrine tumours of the pancreas are rare clinical findings and classified being non-functional or functional. Mostly they occur without any distinct symptoms [2] [8].
In clinical practice, patients with suspected pancreatic lesion receive morphologic imaging as an initial examination procedure [33].
According to 2010 WHO classification, pNETs are graded into G1/G2/G3 related to their mitotic count and Ki-67 index [11].
Six human subtypes of somatostatin receptors have been identified so far; some being overexpressed in pNETs and less common in insulinomas (50-60%), poorly differentiated tumours and somatostatinomas. ^{68}Ga-DOTA-NOC shows high affinity to SSR-2, SSR-3 and SSR-5 [4] [15].

In this retrospective study of 30 patients with histologically confirmed pNETs, who underwent ^{68}Ga-DOTA-NOC PET/CT before or after having received treatment, 20 patients had pathological findings. Each region of interest was semiquantitatively measured with the SUV_{max} of the tracer and a cut-off value (23.27) calculated, showing the highest accuracy at a sensitivity of 100% and specificity of 60%. In the present patient-based and lesion-based sensitivity, specificity and diagnostic accuracy were 100%, respectively. By contrast, the sensitivity of other imaging methods for pNETs like SRS with ^{111}In-octreotide or ^{99m}Tc-HYNIC-TOC, ^{18}F-FDOPA, or ^{18}F-FDG is according to literature much lower. Within the 20 pathological findings, there were significant differences of SUV_{max} with respect to sex, functioning, Ki-67 index, and histological grading in the patient-based analysis.
Generally, it can be stated that the SUV_{max} value is higher in primary pancreatic tumours compared to metastatic lesions in or outside the organ.
The lesion-based analysis showed lower pancreatic SUV_{max} in patients with pathological findings and distant metastases (more in G2 than G1 cases). Higher volume of the lesion was measured on average in primaries.
This study illustrated that any SUV_{max} values lower than 23.27 should be regarded as physiological uptake in the pancreas in patients with well-differentiated pNETs and no distant metastases.

At present, very few studies regarding ^{68}Ga-DOTA-NOC PET/CT in pancreatic neuroendocrine tumours are available. This study should underline the diagnostic value of ^{68}Ga-DOTA-NOC.

One of the benefits of ^{68}Ga-DOTA-NOC is the obtained information about the tumour cell receptors, which is essential for planning targeted radionuclide therapy. Moreover, the fact that this tracer is readily available for nuclear imaging even in centres without an on-site cyclotron makes ^{68}Ga-DOTA-NOC to an attractive and practical tracer for clinical applications in routine. Furthermore, it offers high accuracy, high spatial resolution, can be semi-quantitatively analysed, has lower costs, and convinces with easier examination management.

The SUV_{max} in ^{68}Ga-DOTA-NOC PET/CT is a demonstrated diagnostic parameter in patients with well-differentiated pNETs (G1 and G2) and should be considered in clinical practice to state the diagnosis of pancreatic neuroendocrine tumour. High accuracy and sensitivities were reported in several studies in comparison to other tracers, which were used for somatostatin receptor scintigraphy.

In patients with neuroendocrine cancer of unknown primary, ^{68}Ga-peptide PET/CT is recommended. Double functional imaging with ^{68}Ga-DOTA-NOC PET/CT and ^{18}F-FDG PET/CT, as it efficiently detects high-grade pNETs, may be the best option to detect all histological types of pancreatic NETs.

^{18}F-FDOPA is more suitable for well-differentiated tumours with low or variable somatostatin receptor expression.

Considering that various ^{68}Ga-DOTA-peptides are currently available for pNET imaging and the fact that the appropriate SUV_{max} is not directly comparable, other studies are required to receive cut-off values for comparable positron emitting somatostatin analogue tracers.

Because of the small size of this study population, additional, more extensive trials are needed to reinforce the confirmation of the diagnostic value of ^{68}Ga-DOTA-NOC in patients with neuroendocrine tumour of the pancreas as the gold standard in nuclear medicine imaging.

To sum up, tumour grade and somatostatin receptor status drive the choice of the appropriate tracer in functional nuclear imaging for patients with a neuroendocrine tumour within the pancreas.

8 References

[1] S. Inns and A. Emmanuel, Gastroenterology and hepatology, 2nd ed., Chichester: Wiley Blackwell, 2017, pp. 141-147.

[2] V. Kumar, A. K. Abbas and J. C. Aster, Robbins and Cotran pathologic basis of disease, 9th ed., Philadelphia: Saunders, Elsevier, 2014, pp. 1121-1122.

[3] V. Ambrosini, D. Campana, G. Polverari, C. Peterle, S. Diodato and C. Ricci et al., Prognostic value of 68Ga-DOTA-NOC PET/CT SUVmax in Patients with Neuroendocrine Tumors of the Pancreas, *Journal of Nuclear Medicine,* vol. 56, no. 12, pp. 1843-1848, 8 December 2015.

[4] C. M. Deroose, E. Hindié, E. Kebebew, B. Goichot, K. Pacak and D. Taieb et al., Molecular Imaging of Gastroenteropancreatic Neuroendocrine Tumors: Current Status and Future Directions, *Journal of Nuclear Medicine,* vol. 57, no. 12, pp. 1949-1956, 3 November 2016.

[5] A. Vinik, R. Perry, C. Casellini, M. Hughes and E. Feliberti, Pathophysiology and Treatment of Pancreatic Neuroendocrine Tumors (PNETs): New Developments, E*ndotext,* South Darthmouth (MA): MDText.com, Inc, 2015 PMID25905300.

[6] O. Saint-Marc, A. Cogliandolo, A. Pozzo and R. R. Pidoto, A primary pancreatic carcinoid tumour with unusual clinical complaints : A case report, *World Journal of Surgical Oncology,* no. 2, pp. 1-4, 13 February 2004.

[7] T. Ligiero Braga and R. Santos-Oliviera, PPoma Review: Epidemiology, Aetiopathogenesis, Prognosis and Treatment, *Diseases,* vol. 6, no. 1, p. 8, 11 January 2018.

[8] S. Cingarlini, S. Ortolani, M. Salgarello, G. Butturini, A. Malpaga and V. Malfatti et al., Role of Combined 68Ga-DOTATOC and 18F-FDG Positron Emission Tomography/Computed Tomography in the Diagnostic Workup of Pancreas Neuroendocrine Tumors: Implications for Managing Surgical Decisions, *Pancreas,* vol. 46, no. 1, pp. 42-47, January 2017.

[9] C. Ro, W. Chai, V. E. Yu and R. Yu, Pancreatic neuroendocrine tumors: biology, diagnosis, and treatment, *Chinese Journal of Cancer,* vol. 32, no. 6, pp. 312-324, June 2013.

[10] L. Bubendorf, G. E. Feichter, E. C. Obermann and P. Dalquen, Pathologie, 3rd ed., Berlin, Heidelberg: Springer, Berlin, Heidelberg, 2011, pp. 406-407.

[11] A. Perren, A. Schmitt, P. Komminoth, M. Anlauf and G. Klöppel, Klassifikation und Pathologie gastroenteropankreatischer neuroendokriner Tumoren, *Viszeralmedizin,* vol. 26, pp. 234-240, 19 November 2010.

[12] G. Luo, A. Javed, J. R. Strosberg, K. Jin, Y. Zhang and C. Liu et al., Modified staging classification for pancreatic neuroendocrine tumors on the basis of the American Joint Committee on Cancer and European Neuroendocrine Tumor Society Systems, *Journal of Clinical Oncology,* vol. 35, no. 3, pp. 274-280, September 2017.

[13] G. Klöppel, G. Rindi, A. Perren, P. Komminoth and D. S. Klimstra, The ENETS and AJCC/UICC TNM classifications of the neuroendocrine tumors of the gastrointestinal tract and the pancreas: A statement, *Virchows Archiv,* vol. 456, no. 6, pp. 595-597, June 2010.

[14] S. M. Rizvi, J. Wong, M. W. Saif and Y. Jia, Pharmacogenetics in neuroendocrine tumors of the pancreas, *Journal of Pancreas,* vol. 15, no. 4, pp. 299-302, 28 July 2014.

[15] J. K. Ramage, A. Ahmed, J. Ardill, N. Bax, D. Breen and M. Caplin et al., Guidelines for the management of gastroenteropancreatic neuroendocrine (including carcinoid) tumours (NETs), *Gut,* vol. 61, pp. 6-32, 2012.

[16] B. Katona, G. Roccaro, M. Soulen, Y.-X. Yang, B. Bennett and B. Riff et al., Efficacy of Peptide Receptor Radionuclide Therapy in a United States-Based Cohort of Metastatic Neuroendocrine Tumor Patients, *Pancreas,* vol. 46, no. 9, pp. 1121-1126, October 2017.

[17] K. Öberg, Management of functional neuroendocrine tumors of the pancreas, *Gland Surgery,* vol. 7, no. 1, pp. 20-27, February 2018.

[18] K. L. McCane and S. E. Huether, Study guide for Pathophysiology, 7th ed., St. Louis, Mosby: Elsevier Mosby, 2014, p. 706.

[19] V. Ambrosini, P. Tomassetti, P. Castellucci, D. Campana, G. Montini and D. Rubello et al., Comparison between 68Ga-DOTA-NOC and 18F-DOPA PET for the detection of gastro-entero-pancreatic and lung neuro-endocrine tumours, *European Journal of Nuclear Medicine and Molecular Imaging,* vol. 35, no. 8, pp. 1431-1438, August 2008.

[20] I. Virgolini, V. Ambrosini, J. B. Bomanji, R. Baum, S. Fanti and M. Gabriel et al., Procedure guidlines for PET/CT tumour imaging with 68Ga-DOTA-conjugated

peptides: 68Ga-DOTA-TOC, 68Ga-DOTA-NOC, 68Ga-DOTA-TATE, *European Journal of Nuclear Medicine and Molecular Imaging,* vol. 37, no. 10, pp. 2004-2010, October 2010.

[21] D. Wild, J. Schmitt, M. Ginj, H. Mäcke, B. Bernard and E. Krenning et al., DOTA-NOC, a high affinity ligand of somatostatin receptor subtypes 2, 3 and 5 for labelling with various radiometals, *European Journal of Nuclear Medicine and Molecular Imaging,* vol. 30, no. 10, pp. 1338-1347, October 2003.

[22] puchem.ncbi.nlm.nih.gov, 68Ga-DOTA-NOC, 2015. [Online]. Available: https://pubchem.ncbi.nlm.nih.gov/substance/58086676. [Accessed 18 November 2018].

[23] C. Pettinato, A. Sarnelli, M. Di Donna, S. Civollani, C. Nanni and G. Montini et al., 68Ga-DOTANOC: biodistribution and dosimetry in patients affected by neuroendocrine tumors, *European Journal of Nuclear Medicine and Molecular Imaging,* vol. 35, no. 1, pp. 72-79, january 2008.

[24] IAEA, Production of long lived parent radionuclides for generators: 68Ge, 82Sr, 90Sr and 188W, *IAEA Radioisotopes and Radiopharmaceutical Series No.2,* Vienna 2010.

[25] D. Mueller, I. Klette, R. Baum, M. Gottschaldt, M. Schultz and W. Breeman et al., Simplified NaCl based 68Ga concentration and labeling procedure for rapid synthesis of 68Ga radiopharmaceuticals in high radiochemical purity, *Bioconjugate Chemistry,* vol. 23, no. 8, pp. 1712-1717, 2012.

[26] D. Dwivedi, A. Dwivedi, Snehlata, S. Lochab, R. Kumar and N. Naswa et al., Radiation exposure to nuclear medicine personnel handling positron emitters from Ge-68/Ga-68 generator, *Indian Journal of Nuclear Medicine,* vol. 26, no. 2, pp. 86-90, April 2011.

[27] R. Martin, S. Jüttler, M. Müller and H.-J. Wester, Cationic eluate pretreatment for automated synthesis of [68Ga]CPCR4.2, *Nuclear medicine and biology,* vol. 41, no. 1, pp. 84-89, october 2013.

[28] H. Kvaternik, D. Hausberger, C. Zink, B. Rumpf and R. M. Aigner, 68Ga-peptide preparation with the use of two 68Ge/68Ga-generators, *EJNMMI Radiopharmacy and Chemistry,* no. 1 (Suppl 1), p. 23, june 2016.

[29] Council of Europe, *European Pharmacopoeia,* 9th ed., Strasbourg: Council of Europe, 2018.

[30] IAEA, Quality control in the production of radiopharmaceuticals, *IAEA TECDOC SERIES,* no. 1856, 2018.

[31] W. A. Weber, S. Ziegler, R. Thödtmann, A.-R. Hanauske and M. Schwaiger, Reproducibility of metabolic measurements in malignant tumors using FDG PET, *Journal of Nuclear Medicine,* vol. 40, pp. 1771-1777, 1999.

[32] S. Balogova, J.-N. Talbot, V. Nataf, L. Michaud, V. Huchet and K. Kerrou et al., 18F-fluorodihydroxyphenylalanine vs other radiopharmaceuticals for imaging neuroendocrine tumours according to their type, *European Journal of Nuclear Medicine and Molecular Imaging,* vol. 40, no. 6, pp. 943-66, June 2013.

[33] S. Hoegerle, C. Altehoefer, N. Ghanem, G. Koehler, C. Waller and H. Scheruebl et al., Whole-Body 18FDOPA PET for Detection of Gastrointestinal Carcinoid Tumors, *Radiology,* vol. 220, no. 2, pp. 373-380, july 2001.

[34] H. Schicha and O. Schober, Nuklearmedizin: Basiswissen und klinische Anwendung, 7th ed., Stuttgart: Schattauer, 2013.

[35] S. Kohlfürst, P. Malle and P. Lind, Gastroenteropankreatische Neuroendokrine Tumore, *Wiener klinisches Magazin,* vol. 12, no. 3, pp. 18-23, June 2009.

[36] E. H. Tan and C. H. Tan, Imaging of ganstroenteropancreatic neuroendocrine tumors, *World Journal of Clinical Oncology,* vol. 2, no. 1, pp. 28-43, 2011.

[37] H. R. Balon, S. Goldsmith, B. Siegel, E. Silberstein, E. Krenning and O. Lang et al., Procedure guideline for somatostatin receptor scintigraphy with (111)In-pentetreotide, *Journal of Nuclear Medicine,* vol. 42, no. 7, pp. 1134-8, 2001.

[38] A. Ait Boudaoud, B. Verges, J. Petit, S. Tatulashvili, A. Cochet and O. Humbert, Uptake in the pancreatic uncinate process on the 111In-octreotide scintigraphy: How to distinguish physiological from pathological uptake?, *Nuclear Medicine Communications,* vol. 38, no. 9, pp. 737-743, september 2017.

[39] X. Hou, B. Birkenfeld, H. Piwowarska-Bilska and A. Celler, Patient-specific dosimetry of 99mTc-HYNIC-Tyr3-Octreotide in children, *EJNMMI Physics,* vol. 4, no. 24, pp. 1-13, october 2017.

[40] V. Artiko, D. Sobic-Saranovic, S. Pavlovic, M. Petrovic, M. Zuvela and A. Antic et al., The clinical value of scintigraphy of neuroendocrine tumors using (99m)Tc-HYNIC-TOC, *Journal of the Balkan Union of Oncology,* vol. 17, no. 3, pp. 537-42, 2012.

[41] I. Garai, S. Barna, G. Nagy and A. Forgács, Limitations and pitfalls of 99mTc-EDDA/HYNIC-TOC (Tektrotyd) scintigraphy, *Nuclear medicine review: Central & Eastern Europe,* vol. 19, no. 2, pp. 93-98, july 2016.

[42] K. Liepe and A. Becker, 99mTc-Hynic-TOC imaging in the diagnostic of neuroendocrine tumors, *World Journal of Nuclear Medicine,* vol. 17, no. 3, pp. 151-155, july 2018.

[43] I. Brink, M. Hentschel, H. Neumann, A.-O. Schäfer and E. Moser, FDOPA-PET als Paradigma molekularer Bildgebung in der Onkologie, *Der Nuklearmediziner,* vol. 30, no. 1, pp. 70-82, 2007.

[44] C. Nanni, S. Fanti and D. Rubello, 18F-DOPA PET and PET/CT, *The Journal of Nuclear Medicine,* vol. 48, no. 10, pp. 1577-9, 2007.

[45] K. P. Koopmans, O. C. Neels, I. Kema, P. Elsinga, W. J. Sluiter and K. Vanghillewe et al., Improved Staging of Patients With Carcinoid and Islet Cell Tumors With 18F-Dihydroxy-Phenyl-Alanine and 11C-5-Hydroxy-Tryptophan Positron Emission Tomography, *Journal of Clinical Oncology,* vol. 26, no. 9, pp. 1489-95, march 2008.

[46] W. Mohnike, W. Barthlen, K. Mohnike and O. Blankenstein, Positron emission tomography/computed tomography diagnostics by means of fluorine-18-L-dihydroxyphenylalanine in congenital hyperinsulinism, *Seminars in Pediatric Surgery,* vol. 20, no. 1, pp. 23-27, february 2011.

[47] M. Schiesser, P. Veit-Haibach, M. Muller, M. Weber, P. Bauerfeind, T. Hany and P.-A. Clavien, Value of combined 6-[18F]fluorodihydroxyphenylalanine PET/CT for imaging of neuroendocrine tumours, *British Journal of Surgery,* vol. 97, no. 5, pp. 691-697, march 2010.

[48] R. Boellaard, R. Delgado-Bolton, W. Oyen, F. Giammarile, K. Tatsch and W. Eschner et al., FDG PET/CT: EANM procedure guidelines for tumour imaging: version 2.0, *European Journal of Nuclear Medicine and Molecular Imaging,* vol. 42, no. 2, pp. 328-54, february 2015.

[49] F. Jamar, J. Buscombe, A. Chiti, P. E. Christian, D. Delbeke and K. Donohoe et al., EANM/SNMMI guideline for 18F-FDG use in inflammation and infection, *The Journal of Nuclear Medicine,* vol. 54, no. 4, pp. 647-58, april 2013.

[50] B. Krause, T. Beyer, A. Bockisch, D. Delbeke, J. Kotzerke and V. Minkov et al., FDG-PET/CT in oncology* German guideline, *Nuklearmedizin,* vol. 46, no. 6, pp. 291-301, february 2007.

[51] M. Kitano, C. Millo, R. Rahbari, P. Herscovitch, K. Gesuwan and R. C. Webb et al., Comparison of 6-18F-Fluoro-L-DOPA, 18F-2-deoxy-D-glucose, CT, and MRI in patients with pancreatic neuroendocrine tumors with von Hippel-Lindau disease, *Surgery,* vol. 150, no. 6, pp. 1122-8, december 2011.

[52] C. von Falck, A. Boerner, M. Galanski and W. Knapp, Neuroendocrine tumour of the mediastinum: fusion of 18F-FDG and 68Ga-DOTA-TOC PET/CT datasets demonstrates different degrees of differentiation, *European Journal of Nuclear Medicine and Molecular Imaging,* vol. 34, no. 5, p. 812, 2007.

[53] I. Kayani, J. Bomanji, A. Groves, G. Conway, S. Gacinovic and T. Win et al., Functional imaging of neuroendocrine tumors with combined PET/CT using 68Ga-DOTATATE (Dota-DPhe1, Tyr3-octreotate) and 18F-FDG, *Cancer,* vol. 112, no. 11, pp. 2447-2455, june 2008.

[54] R. Abgral, S. Leboulleux, D. Déandreis, A. Aupérin, J. Lumbroso and C. Dromain et al., Performance of 18Fluorodeoxyglucose-Positron Emission Tomography and Somatostatin Receptor Scintigraphy for High Ki67 (≥10%) Well-Differentiated Endocrine Carcinoma Staging, *The Journal of Clinical Endocrinology & Metabolism,* vol. 96, no. 3, pp. 665-671, march 2011.

[55] S. Sadowski, V. Neychev, C. Millo, J. Shih, N. Nilubol and P. Herscovitch et al., Prospective Study of 68Ga-DOTATATE Positron Emission Tomography/Computed Tomography for Detecting Gastro-Entero-Pancreatic Neuroendocrine Tumors and Unknown Primary Sites, *Journal of Clinical Oncology,* vol. 34, no. 6, p. 588–596, february 2016.

[56] J. Kunikowska, R. Matyskiel, D. Pawlak, R. Mikolajczak and L. Królicki, Somatostatin receptor imaging in patients with neuroendocrine neoplasia: 99mTc-tectrotide SPECT or SPECT/CT with vs 68Ga-DOTATATE PET/CT – impact in clinical decision, *Journal of Nuclear Medicine,* vol. 57, p. 152, 2016.

[57] V. Ambrosini, D. Campana, L. Bodei, C. Nanni, P. Castellucci and V. Allegri et al., 68Ga-DOTANOC PET/CT clinical impact in patients with neuroendocrine tumors, *Journal of Nuclear Medicine,* vol. 51, no. 5, pp. 669-73, 2010.

[58] K. Antwi, M. Fani, G. Nicolas, C. Rottenburger, T. Heye and J. Reubi et al., Localization of Hidden Insulinomas with 68Ga-DOTA-Exendin-4 PET/CT: A Pilot Study, *The Journal of Nuclear Medicine,* vol. 56, no. 7, pp. 1075-1078, july 2015.

[59] V. Ambrosini, D. Campana, C. Nanni, S. Cambioli, P. Tomassetti and D. Rubello et al., Is 68Ga-DOTA-NOC PET/CT indicated in patients with clinical, biochemical or radiological suspicion of neuroendocrine tumour?, *European Journal of Nuclear Medicine and Molecular Imaging,* vol. 39, no. 8, pp. 1278-1283, august 2012.

[60] D. Campana, V. Ambrosini, R. Pezzilli, S. Fanti, A. Labate and D. Santini et al., Standardized uptake values of 68Ga-DOTA-NOC PET: a promising prognostic tool in neuroendocrine tumors, *The Journal of Nuclear Medicine,* vol. 51, no. 3, pp. 353-9, march 2010.

[61] D. Wild, J. B. Bomanji, P. Benkert, H. Maecke, P. J. Ell and J. C. Reubi et al., Comparison of 68Ga-DOTANOC and 68Ga-DOTATATE PET/CT Within Patients with Gastroenteropancreatic Neuroendocrine Tumors, *The Journal of Nuclear Medicine,* vol. 54, no. 3, pp. 364-372, march 2013.

[62] S. Chondrogiannis, M. C. Marzola, A. Al-Nahhas, T. Venkatanarayana, A. Mazza and G. Opocher et al., Normal biodistribution pattern and physiologic variants of 18F-DOPA PET imaging, *Nuclear Medicine Communications,* vol. 34, no. 12, pp. 1141-9, 2013.

[63] A. Imperiale, F. Sebag, M. Vix, F. Castinetti, L. Kessler and F. Moreau et al., 18F-FDOPA PET/CT imaging of insulinoma revisited, *European journal of nuclear medicine and molecular imaging,* vol. 42, no. 3, pp. 409-418, november 2014.